

Prediction-Powered Inference

Anastasios N. Angelopoulos* Stephen Bates* Clara Fannjiang*
Michael I. Jordan* Tijana Zrnic*

University of California, Berkeley

Abstract

We introduce *prediction-powered inference*—a framework for performing valid statistical inference when an experimental data set is supplemented with predictions from a machine-learning system such as AlphaFold. Our framework yields provably valid conclusions without making any assumptions on the machine-learning algorithm that supplies the predictions. Higher accuracy of the predictions translates to smaller confidence intervals, permitting more powerful inference. Prediction-powered inference yields simple algorithms for computing valid confidence intervals for statistical objects such as means, quantiles, and linear and logistic regression coefficients. We demonstrate the benefits of prediction-powered inference with data sets from proteomics, genomics, electronic voting, remote sensing, census analysis, and ecology.

1 Introduction

Machine-learning algorithms are increasingly employed across science and technology as black-box systems that supply predictions to augment or supplant costly experimental measurements. Such machine-learning systems, generally trained on experimental data, can be used to generate predictions for large numbers of entities that were not studied experimentally. For example, predictions of three-dimensional structure can be made for the entire catalog of known proteins [1]. Such predictions can extend our capabilities throughout modern science, in examples such as assessment of molecular activity, tumor prognoses, or microclimatic modeling. Moreover, there is a cumulative effect—chains of predictions can feed further predictions. As such prediction-based science becomes increasingly common, an urgent agenda item is to assess its support in terms of basic principles of statistical inference.

The analysis summarized in Figure 1 substantiates this need. The goal of this analysis is to form a confidence interval for the fraction of the Amazon rainforest that was lost between 2000 and 2015. A small number of gold-standard deforestation labels for certain parcels of land are available, having been collected through field visits, an expensive process not suited for large-area analysis [2]. On the other hand, machine-learning predictions of forest cover are also available, based on satellite imagery, for the entire Amazon [3]. In this setting, there are two natural alternatives for constructing confidence intervals for the true deforestation fraction. The first is to use the predictions as if they were gold-standard labels—an approach that we refer to as the *imputation approach*. The second is to use only the actual gold-standard labels and dispense with the predictions, which we refer to as the *classical approach*. As seen in the figure, the imputation approach yields a small confidence interval that fails to cover the true deforestation fraction. The classical approach does cover the truth at the expense of a wider interval and, accordingly, diminished inferential power. See Appendix E.1 for methodological details.

A second example is shown in Figure 2. Here the goal is to construct a confidence interval for an odds ratio that quantifies a putative association between whether an amino acid residue is phosphorylated and whether it is part of an intrinsically disordered region of the protein. Our data come from Bludau,

* Authors listed alphabetically. Contact: {angelopoulos, stephenbates, claraify, michael.jordan, tijana.zrnic}@berkeley.edu

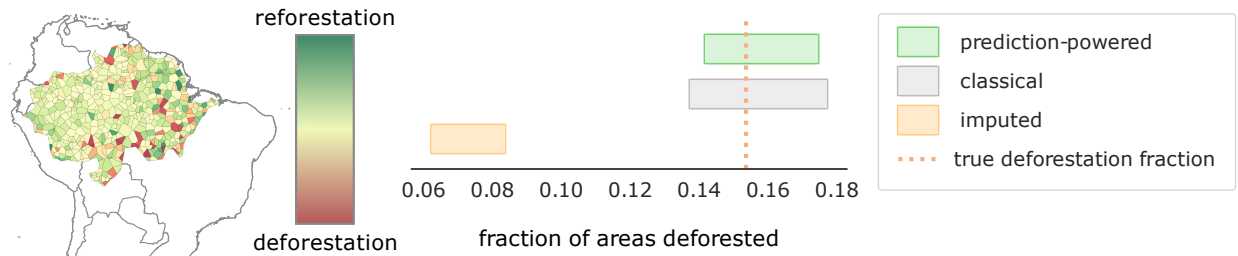


Figure 1: **Forest cover lost in the Amazon rainforest between 2000 and 2015.** The map shows the forest cover change predicted by a machine-learning system using satellite images as input. The prediction-powered interval covers the true fraction of deforested areas, while the imputed interval fails. The classical interval is wider than the prediction-powered interval. The experiment can be reproduced here: [jupyter](#)

Willems, Zeng, Strauss, Hansen, Tanzer, Karayel, Schulman, and Mann [4], who used protein structures predicted by AlphaFold [1] to predict disorder for thousands of residues and then computed an odds ratio assessing association between phosphorylation and disorder. Their methodology was what we refer to as the imputation approach—using the predictions as if they were ground truth. As seen in Figure 2, where we have constructed confidence intervals for a subset of the proteins studied by Bludau et al., the imputation approach significantly overestimates the true odds ratio. Moreover, it does so confidently. As for the classical interval, while it does cover the truth, it is so large that it contains an odds ratio value of one, meaning that the direction of the association is ambiguous. Neither of these inferences is satisfactory. See Section 3.2 for methodological details and further discussion of this experiment.

The current paper asks whether it is possible to get the best of both worlds—to exploit predictions from a machine-learning system while still providing guarantees of statistical validity. We study this question in a general setting with n data points accompanied by gold-standard outcomes or labels and N unlabeled data points whose labels are predicted by a machine-learning model. We assume that N is much larger than n . The setting is reminiscent of a methodology in machine learning known as “semi-supervised learning,” where the idea is to improve the predictions of a model by making use of unlabeled data [5]. Our goal is different. We take the prediction model as pre-existing, as in cases like AlphaFold, where a model was trained offline perhaps at great expense and with massive data. We consider a scientist who wishes to use predictions from the model to perform inference within a scientific inquiry. The scientist’s goal is not to replace the experimental data with predictions, but rather, to leverage the immense number of predictions to improve their confidence in a scientific conclusion. This goal is relevant not only in science but also in many other domains involving consequential decision-making, including medicine, commerce, and policy.

We present *prediction-powered inference*, a framework that provides an affirmative answer to the question

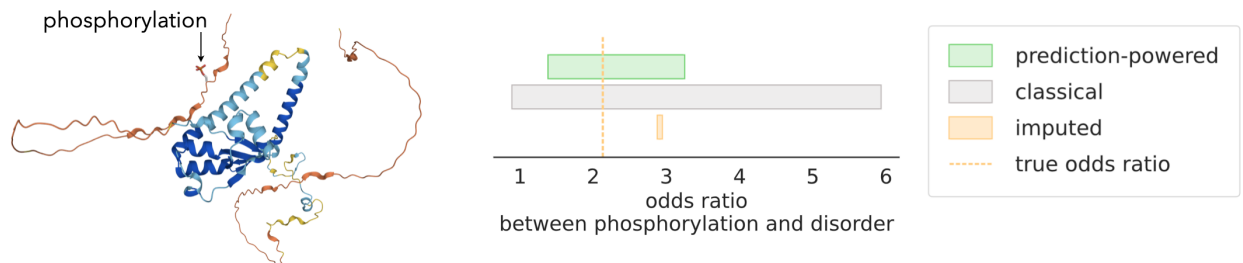


Figure 2: **Quantifying the association between phosphorylation and disorder using AlphaFold.** The left panel shows an example protein colored by the predicted probability of disorder per residue. One residue is phosphorylated. The prediction-powered interval covers the true odds ratio between disorder and phosphorylation, while the imputed one fails. The classical interval is conservative and covers an odds ratio value of one, meaning the direction of association is ambiguous. The experiment can be reproduced here: [jupyter](#)

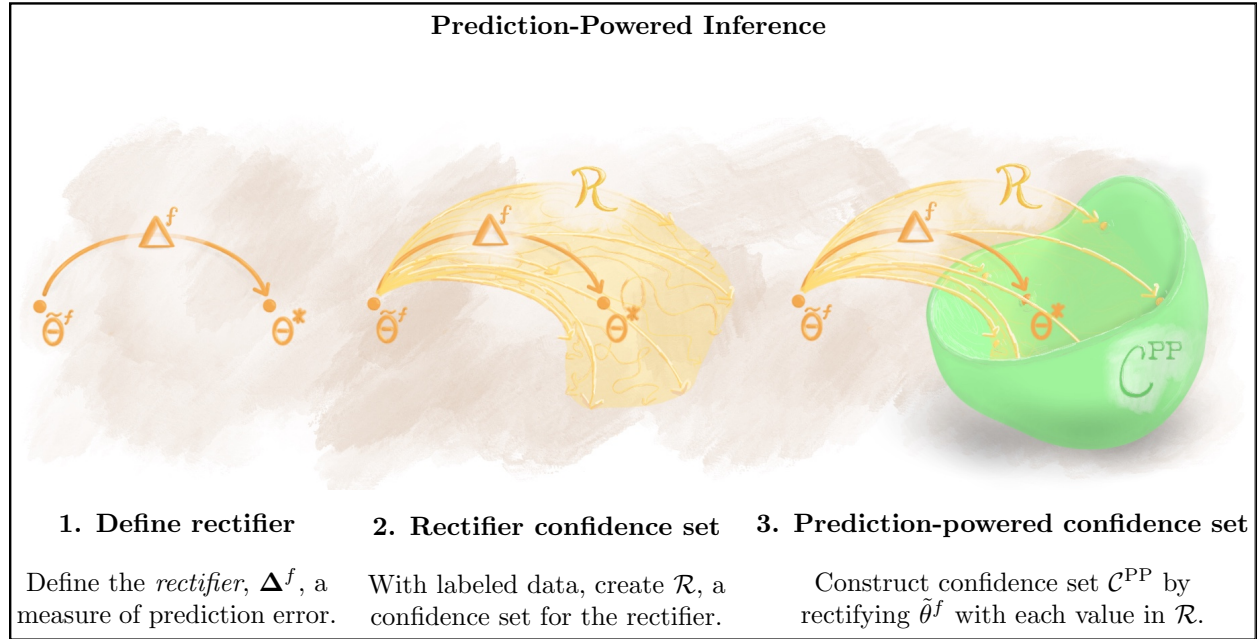
of whether predictions can improve inferential quality. Rather than using predictions as raw data, prediction-powered inference uses the labeled data to estimate a mathematical object that we refer to as the *rectifier*. The rectifier makes it possible to transform parameter estimates based on predictions into a statistically valid confidence set. The effectiveness of prediction-powered inference can be seen in both Figure 1 and Figure 2, where the resulting confidence intervals (in green) not only cover the truth, but also are smaller than those obtained using the classical approach. Notably, in Figure 2, the prediction-powered interval does not contain the value one, permitting a qualitative change in the resulting scientific conclusion.

1.1 General principle

We now overview prediction-powered inference. The goal is to estimate a quantity θ^* , such as the mean or median value of the outcome. Towards this goal, we have access to a small gold-standard data set of paired features and outcomes, $(X, Y) = ((X_1, Y_1), \dots, (X_n, Y_n))$, as well as the features from a large unlabeled data set, $(\tilde{X}, \tilde{Y}) = ((\tilde{X}_1, \tilde{Y}_1), \dots, (\tilde{X}_N, \tilde{Y}_N))$, where we do not observe the true outcomes $\tilde{Y}_1, \dots, \tilde{Y}_N$. We care about the case where $N \gg n$. For both data sets, we have predictions of the outcome made by a machine-learning algorithm f , denoted $f(X) = (f(X_1), \dots, f(X_n))$ and $f(\tilde{X}) = (f(\tilde{X}_1), \dots, f(\tilde{X}_N))$.

Prediction-powered inference builds confidence intervals that are guaranteed to contain θ^* . Imagine we have an estimator $\hat{\theta}$ of θ^* . One feasible but naive way to estimate θ^* , which we call the imputation approach, is to treat the predictions as gold-standard outcomes and compute $\tilde{\theta}^f = \hat{\theta}(\tilde{X}, f(\tilde{X}))$. If the predictions are accurate, meaning $f(\tilde{X}_i) \approx \tilde{Y}_i$, then $\tilde{\theta}^f$ is close to θ^* . However, $\tilde{\theta}^f$ will generally be biased due to errors in the predictions. Instead, our key idea is to use the gold-standard data set to quantify how the prediction errors affect the imputed estimate, and then construct a confidence set for θ^* by adjusting for this effect.

More systematically, the first step is to introduce a problem-specific measure of prediction error called the *rectifier*, denoted as Δ^f . The rectifier captures how errors in the predictions lead to bias in $\tilde{\theta}^f$. Intuitively, Δ^f recovers θ^* by “rectifying” $\tilde{\theta}^f$. The appropriate rectifier depends on the estimand of interest θ^* , and we show how to derive it for a broad class of estimands. Next, we use the gold-standard data to construct a confidence set for the rectifier, \mathcal{R} . Finally, we form a confidence set for θ^* by taking $\tilde{\theta}^f$ and rectifying it with each possible value in the set \mathcal{R} . The collection of these rectified values is the prediction-powered confidence set, \mathcal{C}^{PP} , which is guaranteed to contain θ^* with high probability.



Prediction-powered inference leads to powerful and provably valid confidence intervals and p-values for a broad class of statistical problems, enabling researchers to reliably incorporate machine learning into their analyses. We provide practical algorithms for constructing prediction-powered confidence intervals for means, quantiles, modes, linear and logistic regression coefficients, as well as other targets. For concision, our technical statements and algorithms will focus on constructing confidence intervals; however, note that through the duality between confidence intervals and hypothesis tests, our intervals directly imply valid prediction-powered p-values and hypothesis tests as well.

1.2 Further preliminaries

We use $(X, Y) \in (\mathcal{X} \times \mathcal{Y})^n$ to denote the labeled data set, where $X = (X_1, \dots, X_n)$ and $Y = (Y_1, \dots, Y_n)$. We use the terms “labeled” and “gold-standard” interchangeably. We use analogous notation for the unlabeled data set, $(\tilde{X}, \tilde{Y}) \in (\mathcal{X} \times \mathcal{Y})^N$, where the outcomes \tilde{Y} are not observed. For now we assume that (X, Y) and (\tilde{X}, \tilde{Y}) are i.i.d. samples from a common distribution, \mathbb{P} . We generalize our results to settings with distribution shift and finite populations in Section 4.2 and Appendix A, respectively. By θ^* we denote the estimand of interest, which will typically be an underlying property of \mathbb{P} , such as the mean outcome.

Next, we have a prediction rule, $f : \mathcal{X} \rightarrow \mathcal{Y}$, that is independent of the observed data. For example, it may have been trained on other data independent from both the labeled and the unlabeled data. We let $f_i = f(X_i)$ denote the predictions for the labeled data and $\tilde{f}_i = f(\tilde{X}_i)$ denote the predictions for the unlabeled data. Slightly abusing notation, we let $f = (f_1, \dots, f_n)$ and $\tilde{f} = (\tilde{f}_1, \dots, \tilde{f}_N)$. We will treat $X, Y, \tilde{X}, \tilde{Y}, f, \tilde{f}$ as vectors and matrices where appropriate.

Our key conceptual innovation is the *rectifier* Δ^f —a measure of the prediction rule’s accuracy. We formally define the rectifier in Section 2. We use $\hat{\Delta}^f$ to denote an estimate of the rectifier based on labeled data, which we call the empirical rectifier.

1.3 Warmup: Mean estimation

Before presenting our main results, we use the example of mean estimation to build intuition. Our goal is to give a valid confidence interval for the average outcome, $\theta^* = \mathbb{E}[Y_1]$. The classical estimate of θ^* is the sample average of the outcomes on the labeled data set, $\hat{\theta}^{\text{class}} = \frac{1}{n} \sum_{i=1}^n Y_i$. We construct a prediction-powered estimate, $\hat{\theta}^{\text{PP}}$, and show that it leads to tighter confidence intervals than $\hat{\theta}^{\text{class}}$ if the prediction rule is accurate. Consider

$$\hat{\theta}^{\text{PP}} = \underbrace{\frac{1}{N} \sum_{i=1}^N \tilde{f}_i}_{\hat{\theta}^f} - \underbrace{\frac{1}{n} \sum_{i=1}^n (f_i - Y_i)}_{\hat{\Delta}^f}.$$

The key idea is that if the predictions are accurate, we have $\hat{\Delta}^f \approx 0$ and $\hat{\theta}^{\text{PP}} \approx \frac{1}{N} \sum_{i=1}^N \tilde{Y}_i$, which has a much lower variance than $\hat{\theta}^{\text{class}}$ since $N \gg n$.

Notice $\hat{\theta}^{\text{PP}}$ is unbiased for θ^* and it is a sum of two independent terms. Thus, we can construct 95% confidence intervals for θ^* as

$$\underbrace{\hat{\theta}^{\text{PP}} \pm 1.96 \sqrt{\frac{\hat{\sigma}_{f-Y}^2}{n} + \frac{\hat{\sigma}_{\tilde{f}}^2}{N}}}_{\text{prediction-powered interval}} \quad \text{or} \quad \underbrace{\hat{\theta}^{\text{class}} \pm 1.96 \sqrt{\frac{\hat{\sigma}_Y^2}{n}}}_{\text{classical interval}},$$

where $\hat{\sigma}_Y^2$, $\hat{\sigma}_{f-Y}^2$, and $\hat{\sigma}_{\tilde{f}}^2$ are the estimated variances of the Y_i , $f_i - Y_i$, and \tilde{f}_i , respectively. The prediction-powered confidence interval is better than the classical interval when the model is good. Because $N \gg n$, the width of the prediction-powered interval is primarily determined by the term $\hat{\sigma}_{f-Y}^2$. Furthermore, when the model has small errors, we have $\hat{\sigma}_{f-Y}^2 \ll \hat{\sigma}_Y^2$. Thus, the width of the prediction-powered interval will be smaller than the width of the classical interval. This variance-reduction argument is the reason that

prediction-powered confidence intervals are smaller than their classical counterparts in a broad range of settings beyond mean estimation.

1.4 Related work

From a statistical perspective, our work is related to the broad topic of inference under misspecification, a cornerstone topic that includes seminal contributions such as those by Huber [6], White [7], and Liang and Zeger [8]. We refer the reader to Buja, Brown, Berk, George, Pitkin, Traskin, Zhang, and Zhao [9] for a discussion.

Our technical results generalize tools from the model-assisted survey sampling literature [e.g., 10], which provides methods to improve inference from surveys in the presence of auxiliary information. In particular, the mean estimator in Section 1.3 is the difference estimator, closely related to generalized regression estimators [11]. It has long been recognized that model predictions can be leveraged as auxiliary data [12], and much work has gone into producing asymptotically valid confidence intervals when the predictive model is fit on the same data that is used for inference—see [13] for a recent overview. Our work continues in this vein but focuses on predictive models that are fit on separate data. This allows us to tackle a much wider range of estimands (e.g., minimizers of any convex objective) and give finite-sample inferences without assumptions about the machine-learning model. Secondly, we go beyond random sampling and consider certain forms of distribution shift in this work.

Our setting, in which we have access to some labeled data alongside unlabeled data, also appears in semisupervised learning [e.g., 5, 14]—that literature studies the question of how to improve prediction accuracy with unlabeled data. Our work is also related to the statistical literature on missing data and multiple imputation [e.g., 15]. In contrast to that line of work, our work is fully nonparametric, allowing for arbitrary prediction models and (unknown) data-generating distributions. Thematically, our work is most similar to the work of Wang, McCormick, and Leek [16], who also introduce a method to correct machine-learning predictions for the purpose of subsequent inference. However, our work provides confidence intervals that are provably valid under minimal assumptions about the data-generating distribution, whereas Wang et al. require certain parametric assumptions about the relationship between the prediction model and the true response.

2 Main theory: Convex estimation

Our main contribution is a technique for inference on estimands that can be expressed as the solution to a *convex optimization problem*. In addition to means, this includes medians, other quantiles, linear and logistic regression coefficients, and many other quantities. Formally, we consider estimands of the form

$$\theta^* = \arg \min_{\theta \in \mathbb{R}^p} \mathbb{E}[\ell_\theta(X_1, Y_1)],$$

for a loss function $\ell_\theta : \mathcal{X} \times \mathcal{Y} \rightarrow \mathbb{R}$ that is convex in $\theta \in \mathbb{R}^p$, for some $p \in \mathbb{N}$. Throughout, we take the existence of θ^* as given. If the minimizer is not unique, our method will return a confidence set guaranteed to contain all minimizers. Under mild conditions, convexity ensures that θ^* can also be expressed as the value solving

$$\mathbb{E}[g_{\theta^*}(X_1, Y_1)] = 0, \tag{1}$$

where $g_\theta : \mathcal{X} \times \mathcal{Y} \rightarrow \mathbb{R}^p$ is a subgradient of ℓ_θ with respect to θ . We will call convex estimation problems where θ^* satisfies (1) nondegenerate, and we will later discuss mild conditions that ensure this regularity.

Defining the rectifier. Following the outline in Section 1.1, the first step in prediction-powered inference is to define a rectifier. As in the mean estimation case, the rectifier captures a notion of prediction error. In the general setting of convex estimation problems, the relevant notion of error is the bias of the subgradient g_θ computed using the predictions:

$$\Delta^f(\theta) = \mathbb{E}[g_\theta(X_1, Y_1) - g_\theta(X_1, f_1)]. \tag{2}$$

Rectifier confidence set. The second step is to create a confidence set for the rectifier, $\mathcal{R}_\delta(\theta)$, satisfying

$$P(\Delta^f(\theta) \in \mathcal{R}_\delta(\theta)) \geq 1 - \delta.$$

Because the rectifier is an expectation for each θ , $\mathcal{R}_\delta(\theta)$ can be constructed using standard, off-the-shelf confidence intervals for the mean, which we review in Appendix D.

Prediction-powered confidence set. The final step is to form a confidence set for θ^* . We do so by combining $\mathcal{R}_\delta(\theta)$ with a term that accounts for finite-sample fluctuations due to having N samples. In particular, for every θ , we want a confidence set $\mathcal{T}_{\alpha-\delta}(\theta)$ for $\mathbb{E}[g_\theta(X_1, f_1)]$, satisfying

$$P(\mathbb{E}[g_\theta(X_1, f_1)] \in \mathcal{T}_{\alpha-\delta}(\theta)) \geq 1 - (\alpha - \delta).$$

Again, since $\mathbb{E}[g_\theta(X_1, f_1)]$ is a mean, constructing $\mathcal{T}_{\alpha-\delta}(\theta)$ is easy and can be done with off-the-shelf tools.

We put all the steps together in Theorem 1.

Theorem 1 (Convex estimation). *Suppose that the convex estimation problem is nondegenerate as in (1). Fix $\alpha \in (0, 1)$ and $\delta \in (0, \alpha)$. Suppose that, for any $\theta \in \mathbb{R}^p$, we can construct $\mathcal{R}_\delta(\theta)$ and $\mathcal{T}_{\alpha-\delta}(\theta)$ satisfying*

$$P(\Delta^f(\theta) \in \mathcal{R}_\delta(\theta)) \geq 1 - \delta; \quad P(\mathbb{E}[g_\theta(X_1, f_1)] \in \mathcal{T}_{\alpha-\delta}(\theta)) \geq 1 - (\alpha - \delta).$$

Let $\mathcal{C}_\alpha^{\text{PP}} = \{\theta : 0 \in \mathcal{R}_\delta(\theta) + \mathcal{T}_{\alpha-\delta}(\theta)\}$, where $+$ denotes the Minkowski sum.¹ Then,

$$P(\theta^* \in \mathcal{C}_\alpha^{\text{PP}}) \geq 1 - \alpha.$$

This result means that we can construct a valid confidence set for θ^* , without assumptions about the data distribution or the machine-learning model, for any nondegenerate convex estimation problem. We also present an asymptotic counterpart of Theorem 1 in Appendix B.1.

Most practical problems are nondegenerate (1). For example, if the loss is differentiable for all $\theta \in \mathbb{R}^p$, then the problem is immediately nondegenerate. Furthermore, if the data distribution does not have point masses and, for every θ , $\ell_\theta(x, y)$ is nondifferentiable only for a measure-zero set of (x, y) pairs, then the problem is again nondegenerate.

We have focused on convex estimation problems, since this is a broad class of estimands addressed by prediction-powered inference. Nonetheless, we highlight that the general principles for prediction-powered inference from Section 1.1 are applicable more broadly, and lead to additional results and algorithms for other estimands and some forms of distribution shift; see Section 4 for such extensions.

2.1 Algorithms

In this section we present prediction-powered algorithms for several canonical inference problems. We defer the proofs of their validity to Appendix C. The algorithms rely on confidence intervals derived from the central limit theorem. We implicitly assume the standard, mild regularity conditions required for the asymptotic validity of such intervals, which we overview in Appendix B.3. We also present a parallel set of algorithms that are obtained via nonasymptotic constructions in Appendix B.2. In the algorithms we use $z_{1-\delta}$ to denote the $1 - \delta$ quantile of the standard normal distribution, for $\delta \in (0, 1)$.

Mean estimation. We begin by returning to the problem of mean estimation:

$$\theta^* = \mathbb{E}[Y_1]. \tag{3}$$

The mean can alternatively be expressed as the solution to a convex optimization problem by writing it as the minimizer of the average squared loss:

$$\theta^* = \arg \min_{\theta \in \mathbb{R}} \mathbb{E}[\ell_\theta(Y_1)] = \arg \min_{\theta \in \mathbb{R}} \mathbb{E} \left[\frac{1}{2} (Y_1 - \theta)^2 \right].$$

¹The Minkowski sum of two sets A and B is equal to $\{a + b : a \in A, b \in B\}$.

The squared loss $\ell_\theta(y)$ is differentiable, with gradient equal to $g_\theta(y) = \theta - y$. Applying this in the definition of the rectifier (2), we get $\Delta^f(\theta) \equiv \Delta^f = \mathbb{E}[f_1 - Y_1]$. Note that this rectifier has no dependence on θ . We provide an explicit algorithm for prediction-powered mean estimation and its guarantee in Algorithm 1 and Proposition 1, respectively.

Proposition 1 (Mean estimation). *Let θ^* be the mean outcome (3). Then, the prediction-powered confidence interval in Algorithm 1 has valid coverage: $\liminf_{n, N \rightarrow \infty} P(\theta^* \in \mathcal{C}_\alpha^{\text{PP}}) \geq 1 - \alpha$.*

Quantile estimation. We now turn to quantile estimation. For a pre-specified level $q \in (0, 1)$, we wish to estimate the q -quantile of the outcome distribution:

$$\theta^* = \min \{ \theta : P(Y_1 \leq \theta) \geq q \}. \quad (4)$$

To simplify the exposition, we assume that the distribution of Y_1 does not have point masses; this ensures that the problem is nondegenerate (1), though it is possible to generalize beyond this setting with a standard construction. It is well known [17] that the q -quantile can be expressed in variational form as

$$\theta^* = \arg \min_{\theta \in \mathbb{R}} \mathbb{E}[\ell_\theta(Y_1)] = \arg \min_{\theta \in \mathbb{R}} \mathbb{E}[q(Y_1 - \theta)\mathbb{1}\{Y_1 > \theta\} + (1 - q)(\theta - Y_1)\mathbb{1}\{Y_1 \leq \theta\}],$$

where ℓ_θ is called the quantile loss (or “pinball” loss). The quantile loss has subgradient $g_\theta(y) = q\mathbb{1}\{y > \theta\} - (1 - q)\mathbb{1}\{y \leq \theta\} = q - \mathbb{1}\{y \leq \theta\}$. Plugging the expression for $g_\theta(y)$ into the definition (2), we get the relevant rectifier: $\Delta^f(\theta) = P(f_1 \leq \theta) - P(Y_1 \leq \theta) = \mathbb{E}[\mathbb{1}\{f_1 \leq \theta\} - \mathbb{1}\{Y_1 \leq \theta\}]$. In Algorithm 2 we state an algorithm for prediction-powered quantile estimation; see Proposition 2 for a statement of validity.

Proposition 2 (Quantile estimation). *Let θ^* be the q -quantile (4). Then, the prediction-powered confidence set in Algorithm 2 has valid coverage: $\liminf_{n, N \rightarrow \infty} P(\theta^* \in \mathcal{C}_\alpha^{\text{PP}}) \geq 1 - \alpha$.*

Logistic regression. In logistic regression, the target of inference is defined by

$$\theta^* = \arg \min_{\theta \in \mathbb{R}^d} \mathbb{E}[\ell_\theta(X_1, Y_1)] = \arg \min_{\theta \in \mathbb{R}^d} \mathbb{E}[-Y_1 \theta^\top X + \log(1 + \exp(\theta^\top X_1))], \quad (5)$$

where $Y_1 \in \{0, 1\}$. The logistic loss is differentiable and hence the optimality condition (1) is ensured. Its gradient is equal to $g_\theta(x, y) = -xy + x\mu_\theta(x)$, where $\mu_\theta(x) = 1/(1 + \exp(-x^\top \theta))$ is the predicted mean for point $x \in \mathcal{X}$ based on parameter vector θ . Other generalized linear models (GLMs) have the same gradient form, and thus also optimality condition (1), but for a different mean predictor $\mu_\theta(x)$ (see Chapter 3 of Efron [18]). For example, Poisson regression uses $\mu_\theta(x) = \exp(x^\top \theta)$. In view of our general solution for convex estimation, the rectifier is constant for all θ and equal to $\Delta^f(\theta) \equiv \Delta^f = \mathbb{E}[X_1(f_1 - Y_1)]$. In Algorithm 3 we state a method for prediction-powered logistic regression and in Proposition 3 we provide its guarantee. We use $X_{i,j}$ to denote the j -th coordinate of point X_i . Poisson regression is handled in essentially the same way: concretely, in Algorithm 3 we simply change the choice of $\mu_\theta(x)$ defined in line 5.

Proposition 3 (Logistic regression). *Let θ^* be the logistic regression solution (5). Then, the prediction-powered confidence set in Algorithm 3 has valid coverage: $\liminf_{n, N \rightarrow \infty} P(\theta^* \in \mathcal{C}_\alpha^{\text{PP}}) \geq 1 - \alpha$.*

Linear regression. Finally, we consider inference for linear regression:

$$\theta^* = \arg \min_{\theta \in \mathbb{R}^d} \mathbb{E}[\ell_\theta(X_1, Y_1)] = \arg \min_{\theta \in \mathbb{R}^d} \mathbb{E}[(Y_1 - X_1^\top \theta)^2]. \quad (6)$$

While it is possible to obtain an algorithm for linear regression based on Theorem 1, one can derive a more powerful solution by using the fact that the natural estimator for problem (6) is linear in Y . We exploit these further properties in Algorithm 4 and Proposition 4, where we state a method for prediction-powered linear regression and establish its validity, respectively.

Proposition 4 (Linear regression). *Let θ^* be the linear regression solution (6) and fix $j^* \in [d]$. Then, the prediction-powered confidence interval in Algorithm 4 has valid coverage: $\liminf_{n, N \rightarrow \infty} P(\theta_{j^*}^* \in \mathcal{C}_\alpha^{\text{PP}}) \geq 1 - \alpha$.*

Algorithm 1 Prediction-powered mean estimation

Input: labeled data (X, Y) , unlabeled features \tilde{X} , predictor f , error level $\alpha \in (0, 1)$

- 1: $\hat{\theta}^{\text{PP}} \leftarrow \tilde{\theta}^f - \hat{\Delta}^f := \frac{1}{N} \sum_{i=1}^N \tilde{f}_i - \frac{1}{n} \sum_{i=1}^n (f_i - Y_i)$ ▷ prediction-powered estimator
- 2: $\hat{\sigma}_f^2 \leftarrow \frac{1}{N} \sum_{i=1}^N (\tilde{f}_i - \tilde{\theta}^f)^2$ ▷ empirical variance of imputed estimate
- 3: $\hat{\sigma}_{f-Y}^2 \leftarrow \frac{1}{n} \sum_{i=1}^n (f_i - Y_i - \hat{\Delta}^f)^2$ ▷ empirical variance of empirical rectifier
- 4: $w_\alpha \leftarrow z_{1-\alpha/2} \sqrt{\frac{\hat{\sigma}_{f-Y}^2}{n} + \frac{\hat{\sigma}_f^2}{N}}$ ▷ normal approximation

Output: prediction-powered confidence set $\mathcal{C}_\alpha^{\text{PP}} = (\hat{\theta}^{\text{PP}} \pm w_\alpha)$

Algorithm 2 Prediction-powered quantile estimation

Input: labeled data (X, Y) , unlabeled features \tilde{X} , predictor f , quantile $q \in (0, 1)$, error level $\alpha \in (0, 1)$

- 1: Construct fine grid Θ_{grid} between $\min_{i \in [N]} \tilde{f}_i$ and $\max_{i \in [N]} \tilde{f}_i$
- 2: **for** $\theta \in \Theta_{\text{grid}}$ **do**
- 3: $\hat{\Delta}^f(\theta) \leftarrow \frac{1}{n} \sum_{i=1}^n (\mathbb{1}\{f_i \leq \theta\} - \mathbb{1}\{Y_i \leq \theta\})$ ▷ empirical rectifier
- 4: $\hat{F}(\theta) \leftarrow \frac{1}{N} \sum_{i=1}^N \mathbb{1}\{\tilde{f}_i \leq \theta\}$ ▷ imputed CDF
- 5: $\hat{\sigma}_\Delta^2(\theta) \leftarrow \frac{1}{n} \sum_{i=1}^n \left(\mathbb{1}\{f_i \leq \theta\} - \mathbb{1}\{Y_i \leq \theta\} - \hat{\Delta}^f(\theta) \right)^2$ ▷ empirical variance of empirical rectifier
- 6: $\hat{\sigma}_f^2(\theta) \leftarrow \frac{1}{N} \sum_{i=1}^N \left(\mathbb{1}\{\tilde{f}_i \leq \theta\} - \hat{F}(\theta) \right)^2$ ▷ empirical variance of imputed CDF
- 7: $w_\alpha(\theta) \leftarrow z_{1-\alpha/2} \sqrt{\frac{\hat{\sigma}_\Delta^2(\theta)}{n} + \frac{\hat{\sigma}_f^2(\theta)}{N}}$ ▷ normal approximation

Output: prediction-powered confidence set $\mathcal{C}_\alpha^{\text{PP}} = \left\{ \theta \in \Theta_{\text{grid}} : |\hat{F}(\theta) - \hat{\Delta}^f(\theta) - q| \leq w_\alpha(\theta) \right\}$

Algorithm 3 Prediction-powered logistic regression

Input: labeled data (X, Y) , unlabeled features \tilde{X} , predictor f , error level $\alpha \in (0, 1)$

- 1: Construct fine grid $\Theta_{\text{grid}} \subset \mathbb{R}^d$ of possible coefficients
- 2: $\hat{\Delta}_j^f \leftarrow \frac{1}{n} \sum_{i=1}^n X_{i,j} (f_i - Y_i)$, $j \in [d]$ ▷ empirical rectifier
- 3: $\hat{\sigma}_{\Delta,j}^2 \leftarrow \frac{1}{n} \sum_{i=1}^n \left(X_{i,j} (f_i - Y_i) - \hat{\Delta}_j^f \right)^2$, $j \in [d]$ ▷ empirical variance of empirical rectifier
- 4: **for** $\theta \in \Theta_{\text{grid}}$ **do**
- 5: $\hat{g}_j^f(\theta) \leftarrow \frac{1}{N} \sum_{i=1}^N \tilde{X}_{i,j} \left(\mu_\theta(\tilde{X}_i) - \tilde{f}_i \right)$, $j \in [d]$, where $\mu_\theta(x) = \frac{1}{1 + \exp(-x^\top \theta)}$ ▷ imputed gradient
- 6: $\hat{\sigma}_{g,j}^2(\theta) \leftarrow \frac{1}{N} \sum_{i=1}^N \left(\tilde{X}_{i,j} (\mu_\theta(\tilde{X}_i) - \tilde{f}_i) - \hat{g}_j^f(\theta) \right)^2$, $j \in [d]$ ▷ empirical variance of imputed gradient
- 7: $w_{\alpha,j}(\theta) \leftarrow z_{1-\alpha/(2d)} \sqrt{\frac{\hat{\sigma}_{\Delta,j}^2}{n} + \frac{\hat{\sigma}_{g,j}^2(\theta)}{N}}$, $j \in [d]$ ▷ normal approximation

Output: prediction-powered confidence set $\mathcal{C}_\alpha^{\text{PP}} = \left\{ \theta \in \Theta_{\text{grid}} : |\hat{g}_j^f(\theta) + \hat{\Delta}_j^f| \leq w_{\alpha,j}(\theta), \forall j \in [d] \right\}$

Algorithm 4 Prediction-powered linear regression

Input: labeled data (X, Y) , unlabeled features \tilde{X} , predictor f , coefficient $j^* \in [d]$, error level $\alpha \in (0, 1)$

- 1: $\hat{\theta}^{\text{PP}} \leftarrow \tilde{\theta}^f - \hat{\Delta}^f := \tilde{X}^\top \tilde{f} - X^\top (f - Y)$ ▷ prediction-powered estimator
- 2: $\tilde{\Sigma} \leftarrow \frac{1}{N} \tilde{X}^\top \tilde{X}$, $\tilde{M} \leftarrow \frac{1}{N} \sum_{i=1}^N (\tilde{f}_i - \tilde{X}_i^\top \tilde{\theta}^f)^2 \tilde{X}_i \tilde{X}_i^\top$
- 3: $\tilde{V} \leftarrow \tilde{\Sigma}^{-1} \tilde{M} \tilde{\Sigma}^{-1}$ ▷ “sandwich” variance estimator for imputed estimate
- 4: $\Sigma \leftarrow \frac{1}{n} X^\top X$, $M \leftarrow \frac{1}{n} \sum_{i=1}^n (f_i - Y_i - X_i^\top \hat{\Delta}^f)^2 X_i X_i^\top$
- 5: $V \leftarrow \Sigma^{-1} M \Sigma^{-1}$ ▷ “sandwich” variance estimator for empirical rectifier
- 6: $w_\alpha \leftarrow z_{1-\alpha/2} \sqrt{\frac{V_{j^*j^*}}{n} + \frac{\tilde{V}_{j^*j^*}}{N}}$ ▷ normal approximation

Output: prediction-powered confidence set $\mathcal{C}_\alpha^{\text{PP}} = (\hat{\theta}_{j^*}^{\text{PP}} \pm w_\alpha)$

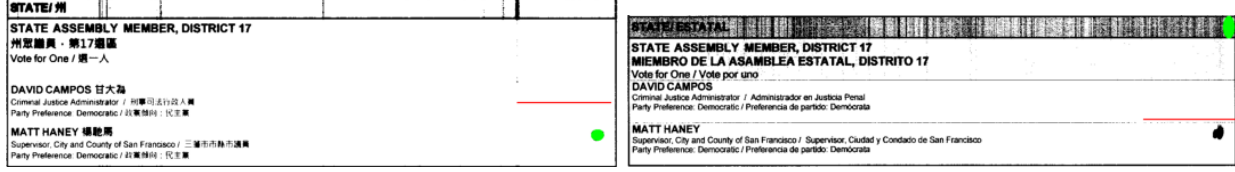


Figure 3: **Examples of ballots** correctly and incorrectly classified. The raw ballot is black and white, the voter’s marking is automatically identified by a computer vision algorithm with a green annotation, and markings below the red line annotation will be considered votes for Matt Haney (and vice versa). The instructional portion of the ballots was cropped out.

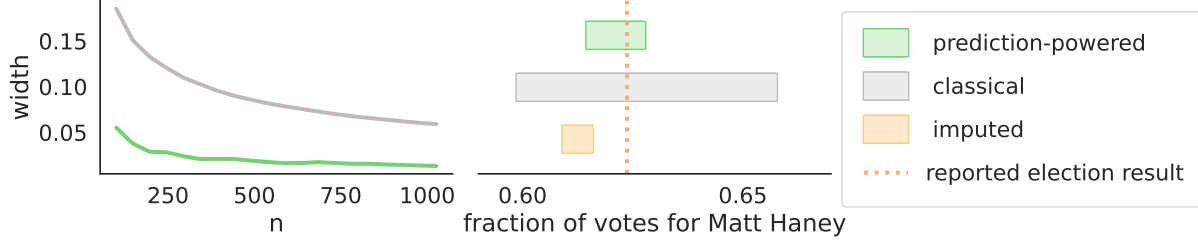


Figure 4: **Election results** produced by prediction-powered inference and the classical and imputed baselines at level 95%. Left: width of intervals as a function of n . Right: confidence intervals with $n = 1024$.

3 Applications

In this section we demonstrate prediction-powered inference on real tasks. In each of the following applications, we compute the prediction-powered confidence interval for an estimand of interest and compare it to two alternatives: the classical interval, which uses only the gold-standard data (X, Y) , and the imputed interval, which uses only the imputed data (\tilde{X}, \tilde{f}) by treating it as gold-standard data. In all cases, we show that the imputed interval, which does not account for the prediction errors, does not contain the true value of the estimand. For the two intervals that are guaranteed to be valid—prediction-powered and classical—we compare their widths as a function of n , the amount of labeled data used.

All code is available at this link. Each example also comes with a corresponding Jupyter notebook that can be accessed by clicking these icons: . We packaged the data in such a way that the reader can run the notebooks on their local machine without downloading large data sets.

3.1 Auditing electronic voting

We studied audits of electronic voting in an election with two candidates. Specifically, we aimed to construct a confidence interval for the proportion of people voting for each candidate using a small number of hand-counted ballots and a large number of ballots read with an optical scanner. On Election Day in the United States, most voters use electronic or optical-scan ballots [19], neither of which are perfectly accurate. Our data were taken from a special election in San Francisco for the Assembly District 17 seat on April 19, 2022. The candidates were David Campos and Matt Haney. We constructed a prediction-powered confidence interval using an optical ballot labeling system and a small number of ballots which we labeled ourselves. This is an example of a *risk-limiting audit*—a statistically valid way to check the results of an election by inspecting subsets of ballots [see, e.g., 20].

Formally, we have $N = 78150$ images of paper ballots $\tilde{X}_i \in \mathcal{X}$, $i \in [N]$, taken using an optical ballot scanner. Each ballot has an associated ground-truth binary vote, $\tilde{Y}_i \in \{0, 1\}$, $i \in [N]$, where a “1” indicates a vote for Matt Haney and a “0” indicates a vote for David Campos. The target of inference is the fraction of votes for Matt Haney, $\theta^* = \mathbb{E}[\tilde{Y}_1]$. To compute the intervals, we hand-annotated $n = 1024$ randomly sampled

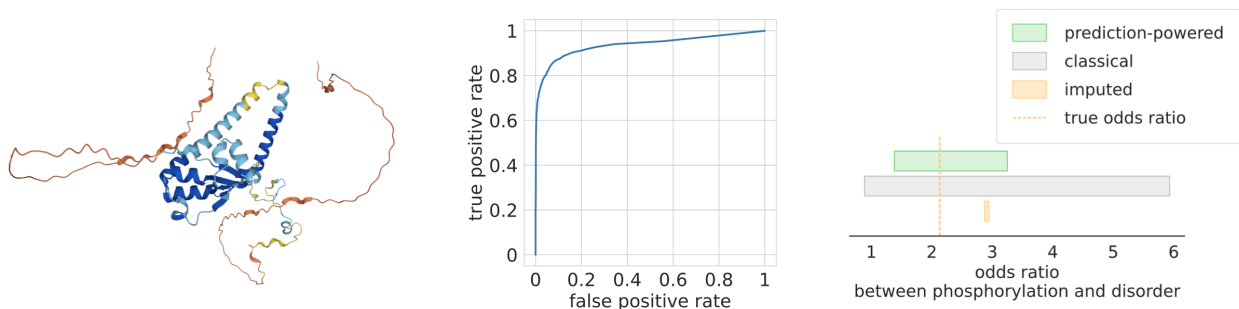


Figure 5: **AlphaFold-based prediction of disorder.** Left: predicted disorder for one example protein (UniProt S5FZ81), colored by predicted probability of disorder per position. Middle: ROC curve of disorder prediction based on AlphaFold structure. Right: confidence interval for the odds ratio between disorder and phosphorylation (type of PTM) produced by prediction-powered inference and the classical and imputed baselines, when $n = 571$. Unlike the classical interval, the prediction-powered interval excludes the value of one and thus the direction of the association is unambiguous.

ballots and imputed labels using a computer vision algorithm $f : \mathcal{X} \rightarrow \{0, 1\}$, representing an optical-ballot scanner. The accuracy of f is 99%, and it is biased towards Matt Haney due to printing errors in the ballots; see Figure 3 for examples. We used Algorithm 1 to construct the prediction-powered confidence interval, and binomial confidence intervals for the imputed and classical baselines. The prediction-powered interval has roughly 1/4 the width of its classical counterpart, and the interval based on imputation is invalid—it does not cover the ground truth. See Figure 4.

3.2 Relating protein structure and post-translational modifications

We demonstrate how prediction-powered confidence intervals for the mean can be used to construct confidence intervals for more elaborate estimands, in particular the odds ratio, which is commonly used to quantify associations between binary random variables.

The goal of the analysis in this section is to characterize the structural context of post-translational modifications (PTMs), which are biochemical modifications of specific positions of a protein sequence that play important regulatory roles. One question of interest is whether PTMs occur more frequently in particular contexts within a protein’s three-dimensional structure, such as intrinsically disordered regions (IDRs), segments of a protein that do not abide in a fixed three-dimensional structure. Recently, Bludau, Willems, Zeng, Strauss, Hansen, Tanzer, Karayel, Schulman, and Mann [4] studied this relationship on an unprecedented proteome-wide scale by using AlphaFold-predicted structures [1] to predict IDRs, in contrast to previous work which considered far fewer experimentally derived structures.

We will refer to a position of a protein sequence being/not being in an IDR as “disordered”/“ordered”, and having/not having a PTM as “modified”/“unmodified.” Let $Y_i \in \{1, 0\}$ denote the gold-standard label of whether or not a position is disordered, and let $Z_i \in \{1, 0\}$ denote whether or not a position is modified. Following Bludau, Willems, Zeng, Strauss, Hansen, Tanzer, Karayel, Schulman, and Mann [4], we obtain a prediction for Y_i , denoted $f_i \in \{1, 0\}$, based on the protein structure predicted by AlphaFold. To quantify the association between PTMs and IDRs, Bludau et al. computed the odds ratio between f_i and Z_i on a data set of hundreds of thousands of protein sequence positions. Though some of the data points also contained a gold-standard label, Y_i , Bludau, Willems, Zeng, Strauss, Hansen, Tanzer, Karayel, Schulman, and Mann [4] did not use these labels in their analyses to avoid dealing with conflicts between labels and predictions. Here, we show how to use both labels and predictions to give confidence intervals for the odds ratio that are valid, in contrast to intervals based only on f_i , and smaller than intervals obtained only using Y_i .

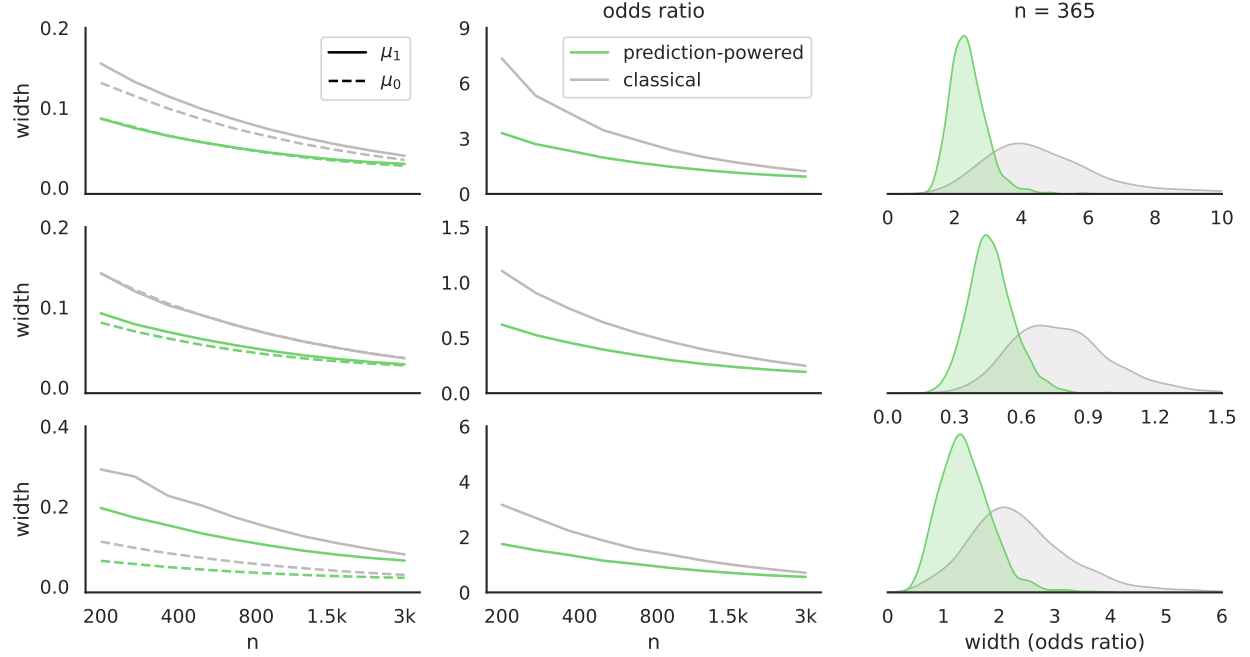


Figure 6: **Odds ratio for three different PTMs**, phosphorylation (top row), ubiquitination (middle row), and acetylation (bottom row). Left: widths of prediction-powered and classical confidence intervals for μ_1 (solid line) and μ_0 (dashed line). Middle: widths of prediction-powered and classical confidence intervals for the odds ratio. Right: distribution of interval widths for the odds ratio when $n = 365$.

The odds ratio between Y_i and Z_i can be written as a function of two means:

$$\theta^* = \frac{\mu_1/(1-\mu_1)}{\mu_0/(1-\mu_0)}, \quad (7)$$

where $\mu_1 = P(Y = 1 | Z = 1)$ and $\mu_0 = P(Y = 1 | Z = 0)$. We therefore proceed by constructing $1 - \alpha/2$ prediction-powered confidence intervals for μ_0 and μ_1 , denoted $\mathcal{C}_0^{\text{PP}} = [l_0, u_0]$ and $\mathcal{C}_1^{\text{PP}} = [l_1, u_1]$, respectively. We then propagate $\mathcal{C}_0^{\text{PP}}$ and $\mathcal{C}_1^{\text{PP}}$ through the odds-ratio formula (7) to get the following confidence interval:

$$\mathcal{C}^{\text{PP}} = \left\{ \frac{c_1}{1-c_1} \cdot \frac{1-c_0}{c_0} : c_0 \in \mathcal{C}_0^{\text{PP}}, c_1 \in \mathcal{C}_1^{\text{PP}} \right\} = \left(\frac{l_1}{1-l_1} \cdot \frac{1-u_0}{u_0}, \frac{u_1}{1-u_1} \cdot \frac{1-l_0}{l_0} \right).$$

By a union bound, \mathcal{C}^{PP} contains θ^* with probability at least $1 - \alpha$. We set $\alpha = 0.1$.

We have 10803 data points from [4], from which we simulated labeled and unlabeled data sets as follows. For each of 1000 trials, we randomly sampled n points to serve as the labeled data set and used the remaining $N = 10803 - n$ points as the unlabeled data set, where we do not observe the labels. For all values of n and all three different types of PTMs that we examined, the prediction-powered confidence intervals are smaller than classical intervals; see Figure 6. Often, the classical intervals are large enough that they contain the odds ratio value of one, as demonstrated in Figure 5, which means the direction of the association cannot be determined from the confidence interval. On the other hand, the imputed confidence interval is far too small and significantly overestimates the true odds ratio; see Figure 5.

3.3 Relationship between age, sex, and income

We next used census data to investigate the quantitative effects of age and sex on income by constructing confidence intervals for the linear regression coefficients relating age (1-99) and sex (M/F) to income. As

can be seen in Figure 7, which plots the distribution of income across sex and different age ranges, income generally increases with age, and men earn more than women in every age category.

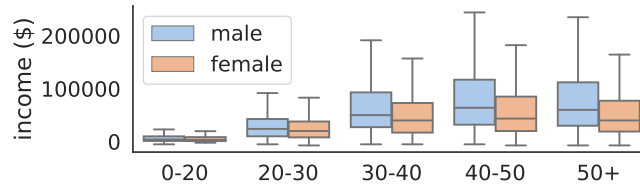


Figure 7: **Distribution of income stratified by age and sex** in the census year 2019.

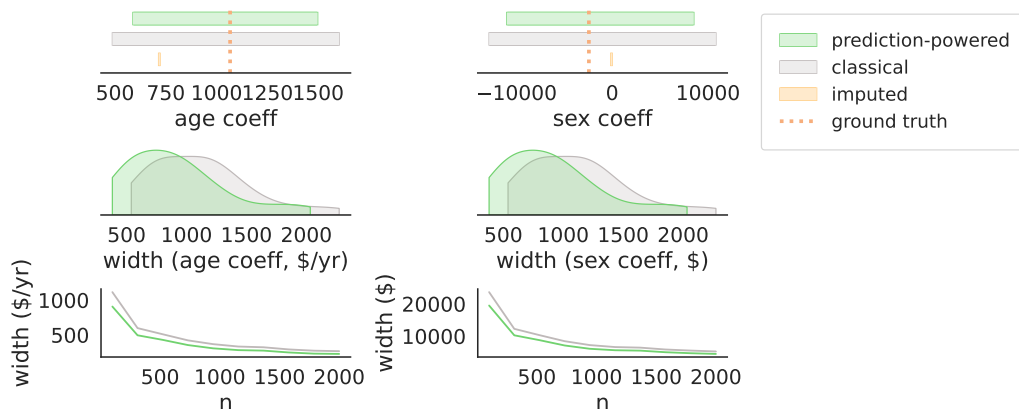


Figure 8: **Confidence intervals at the 95% level** are smaller using prediction-powered inference. Top: confidence intervals with $n = 100$. Middle: density of interval width with $n = 100$. Bottom: average width as a function of n .

Concretely, we used the Folktables interface [21] to download census data from California in the year 2018 (377575 people), including yearly income (\$), and ten covariates including age and sex. On this data, we trained an XGBoost model [22] to predict yearly income from the covariates. Then, in the year 2019 ($N = 378817$ people), we observed all the covariates but only a small number $n = 100$ of yearly incomes. Using the model, we imputed the remaining yearly incomes from the covariates, and then regressed age and sex to the imputed yearly incomes using ordinary least squares. We then formed a prediction-powered confidence interval for the regression parameters using Algorithm 4. The classical and imputed baselines used standard least-squares confidence intervals. See Figure 8 for results. Note that income is difficult to predict, as evidenced by the width of the boxplots in Figure 7, so the prediction-powered interval provides only a moderate improvement over the classical interval. Critically, however, it yields this improvement without succumbing to the overconfidence exhibited by the imputed interval.

3.4 Relationship between income and private health insurance

Again using census data, we studied the effect of income on the procurement of private health insurance. In particular, we fit a logistic regression relating an individual's income to the probability they have private health insurance. Generally, the higher a person's income, the more likely they are to have private health insurance.

The setup is essentially the same as in Section 3.3: we used the Folktables interface to download California census data on income, a binary indicator of private health insurance, and other predictive covariates. We used XGBoost to impute the predictions, and Algorithm 3 to construct the intervals; see Figure 9 for results.

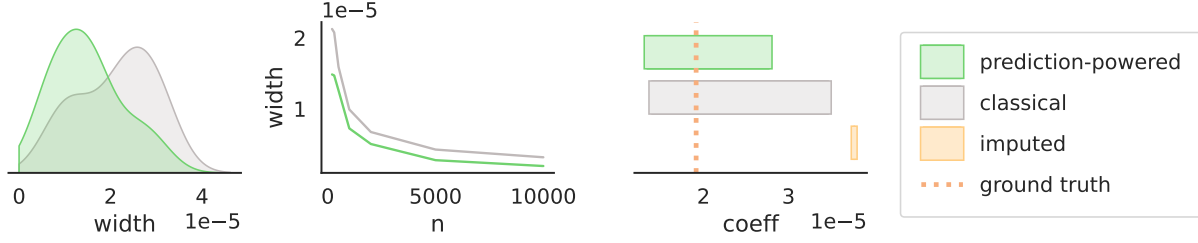


Figure 9: **Confidence intervals for the logistic regression coefficient** relating income and private health insurance coverage at the 95% level. Left: distribution of interval widths with $n = 200$. Middle: mean width as a function of n . Right: intervals with $n = 200$.

3.5 Distribution of gene expression levels

In this section, we demonstrate the construction of prediction-powered confidence intervals on quantiles for studying the effects of regulatory DNA on gene expression. In particular, we aim to characterize the distribution of gene expression levels induced by a population of promoters—regulatory DNA sequences that control how frequently a gene is transcribed. Recently, Vaishnav, Boer, Molinet, Yassour, Fan, Adiconis, Thompson, Levin, Cubillos, and Regev [23] trained a state-of-the-art transformer model on tens of millions of random promoter sequences with the goal of predicting the expression level of a particular gene induced by a promoter sequence (see Figure 10). They then used the model’s predictions to study the effects of promoters—for example, by assessing how quantiles of predicted expression levels differ between different populations of promoters, and verifying those observations by experimentally measuring the expression levels of the promoters of interest.

Let X_i be an 80-base-pair promoter sequence for a particular gene, and let $Y_i \in [0, 20]$ denote the average of replicate ordinal measurements of expression level it causes for the yellow fluorescent protein gene. Furthermore, let $f_i \in [0, 20]$ denote the corresponding expression level predicted by the transformer model in [23]. We focus on estimating the 0.25-, 0.5-, and 0.75-quantiles of expression levels induced by native yeast promoters—promoter sequences that are naturally found in the genomes of *S. cerevisiae*.

We have $N = 61150$ labeled native yeast promoter sequences from [23], from which we simulated labeled and unlabeled data sets as follows. For each of 1000 trials, we randomly sampled n points to serve as the labeled data set and used the remaining $N = 61150 - n$ points as the unlabeled data set. We then used Algorithm 2 to construct prediction-powered intervals with $\alpha = 0.1$. The prediction-powered confidence

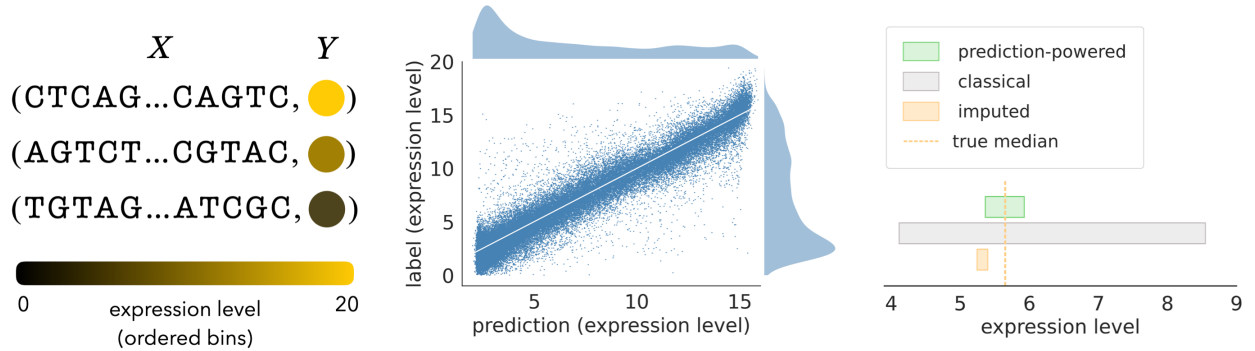


Figure 10: **Predicting gene expression levels from a promoter sequence** [23]. Left: each data point consists of a promoter X_i and an expression level Y_i . Middle: predictive performance of the transformer model on the native yeast promoters used in our experiments (RMSE 2.18, Pearson 0.963, Spearman 0.946). Right: confidence intervals for the median native yeast promoter expression level with $n = 75$ and $\alpha = 0.1$.

intervals for all three quantiles are much smaller than the classical intervals for all value of n ; see Figure 11.

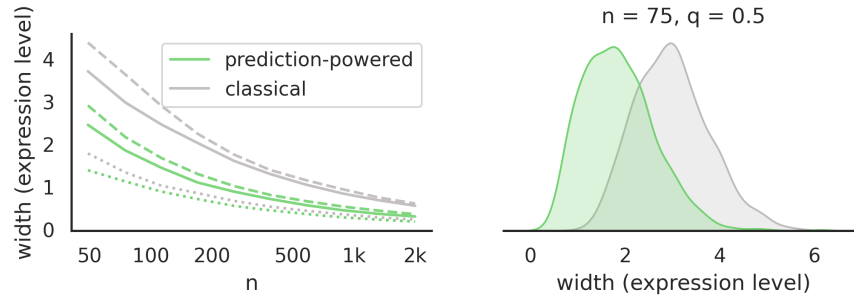


Figure 11: **Widths of confidence intervals around the median** using the transformer model of expression level developed by Vaishnav, Boer, Molinet, Yassour, Fan, Adiconis, Thompson, Levin, Cubillos, and Regev [23]. Left: average width of prediction-powered and classical confidence intervals for the 0.25-quantile (dashed lines), 0.5-quantile (solid lines), and 0.75-quantile (dotted lines). Right: distribution of confidence interval widths for the median using $n = 75$.

3.6 Counting plankton

We counted the number of plankton observed by the Imaging FlowCytobot [24, 25], an automated, submersible flow cytometry system, at Woods Hole Oceanographic Institution in the year 2014. We also had access to data from previous years, which we treated as labeled, and the 2014 data were fully imputed. The resulting confidence interval does not assume that the 2014 data are identically distributed to the data from previous years; we explicitly adjust for the fact that the probability of observing a plankton may change using the label shift technique from Section 4.2.

More formally, our inputs \tilde{X}_i are images taken by the flow cytometry system and the labels \tilde{Y}_i are one of $\{\text{detritus, plankton}\}$, where detritus represents unspecified organic matter; see Figure 12 for examples. We are interested in the number of plankton in the year 2014. For the machine-learning algorithm, we fine-tune an ImageNet pretrained ResNet-152 [26] on labeled data from the years 2006-2012 (2812527 data points). The labeled data set consists of $n = 421238$ image-label pairs from 2013 that the model was not trained on. Finally, we received $N = 329832$ unlabeled images \tilde{X}_i from the new year that has undergone a label

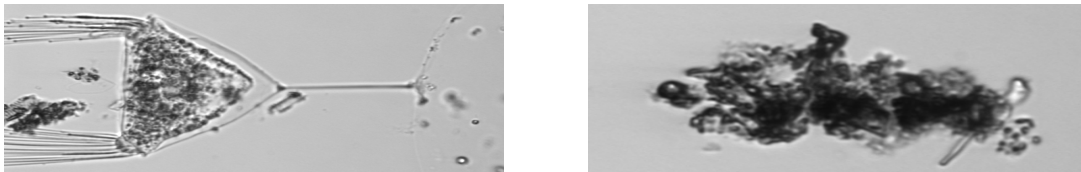


Figure 12: **Examples of plankton and detritus**, respectively.

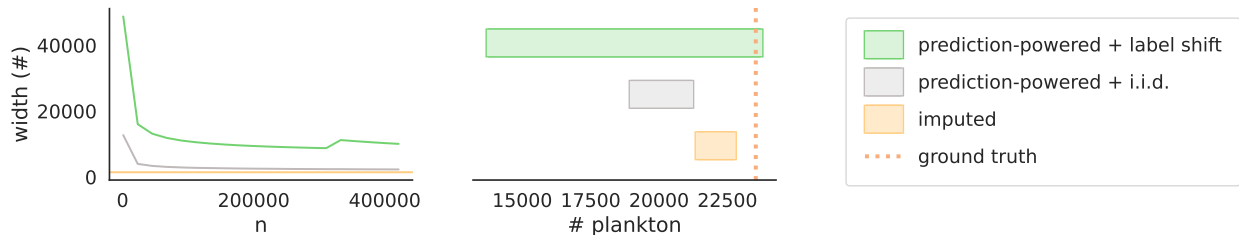


Figure 13: **Confidence intervals on the number of plankton** observed in 2014 at the 95% level. Left: mean width as a function of n . Right: confidence intervals with $n = 421238$.

shift. Given these three ingredients, we used the technique in Section 4.2 to construct the prediction-powered confidence interval on the frequency of observed plankton, while accounting for the distribution shift. We then propagated the confidence interval into a count. See Figure 13 for results. Note that assuming the data is i.i.d. and applying Algorithm 1 for mean estimation results in biased inferences, as does the imputed baseline using a classical binomial confidence interval.

4 Extensions

We demonstrate that the framework of prediction-powered inference is applicable beyond the setting of i.i.d. convex estimation studied in Section 2. First, we provide a strategy for prediction-powered inference when θ^* can be expressed as the optimum of any optimization problem, not necessarily a convex one. Then, we discuss prediction-powered inference under certain forms of distribution shift.

4.1 Beyond convex estimation

The tools developed in Section 2 were tailored to unconstrained convex optimization problems. In general, however, inferential targets can be defined in terms of nonconvex losses or they may have (possibly even nonconvex) constraints. For such general optimization problems, we cannot expect the condition (1) to hold. In this section we generalize our approach to a broad class of risk minimizers:

$$\theta^* = \arg \min_{\theta \in \Theta} \mathbb{E}[\ell_\theta(X_1, Y_1)], \quad (8)$$

where $\ell_\theta : \mathcal{X} \times \mathcal{Y} \rightarrow \mathbb{R}$ is a possibly nonconvex loss function and Θ is an arbitrary set of admissible parameters. As before, if θ^* is not a unique minimizer, our method will return a set that contains all minimizers.

The problem (8) subsumes all previously studied settings. Indeed, when the loss ℓ_θ is convex and subdifferentiable and $\Theta = \mathbb{R}^p$ for some p —which is the case for all problems previously studied— θ^* can be equivalently characterized via the condition (1). In this section we provide a solution that can handle problems of the form (8) in full generality. We note, however, that the solution does not reduce to the one in Section 2 for convex estimation problems, and we expect the method from Section 2 to be more powerful for convex estimation problems with low-dimensional rectifiers.

To correct the imputation approach, we rely on the following rectifier:

$$\Delta^f(\theta) = \mathbb{E}[\ell_\theta(X_1, Y_1) - \ell_\theta(X_1, f_1)]. \quad (9)$$

Notice that the rectifier (9) is always one-dimensional, while the rectifier (2) was p -dimensional.

One key difference relative to the approach of Section 2 is that we have an additional step of data splitting. We need the additional step because, unlike in convex estimation where we know $\mathbb{E}[g_{\theta^*}(X_1, Y_1)] = 0$, for general problems we do not know the value of $\mathbb{E}[\ell_{\theta^*}(X_1, Y_1)]$. To circumvent this issue, we estimate $\mathbb{E}[\ell_{\theta^*}(X_1, Y_1)]$ by approximating θ^* with an imputed estimate on the first $N/2$ unlabeled data points (for simplicity take N to be even). To state the main result, we define

$$\tilde{\theta}^f = \arg \min_{\theta \in \Theta} \frac{2}{N} \sum_{i=1}^{N/2} \ell_\theta(\tilde{X}_i, \tilde{f}_i), \quad \tilde{L}^f(\theta) := \frac{2}{N} \sum_{i=N/2+1}^N \ell_\theta(\tilde{X}_i, \tilde{f}_i).$$

Theorem 2 (General risk minimization). *Fix $\alpha \in (0, 1)$ and $\delta \in (0, \alpha)$. Suppose that, for any $\theta \in \Theta$, we can construct $(\mathcal{R}_{\delta/2}^l(\theta), \mathcal{R}_{\delta/2}^u(\theta))$ and $\mathcal{T}_{\alpha-\delta}(\theta)$ such that*

$$\begin{aligned} P\left(\Delta^f(\theta) \leq \mathcal{R}_{\delta/2}^u(\theta)\right) &\geq 1 - \delta/2; & P\left(\Delta^f(\theta) \geq \mathcal{R}_{\delta/2}^l(\theta)\right) &\geq 1 - \delta/2; \\ P\left(\tilde{L}^f(\theta) - \mathbb{E}[\ell_\theta(X_1, f_1)] \leq \mathcal{T}_{\alpha-\delta}(\theta)\right) &\geq 1 - (\alpha - \delta). \end{aligned}$$

Let

$$\mathcal{C}_\alpha^{\text{PP}} = \left\{ \theta \in \Theta : \tilde{L}^f(\theta) \leq \tilde{L}^f(\tilde{\theta}^f) - \mathcal{R}_{\delta/2}^l(\theta) + \mathcal{R}_{\delta/2}^u(\tilde{\theta}^f) + \mathcal{T}_{\alpha-\delta}(\theta) \right\}.$$

Then, we have

$$P(\theta^* \in \mathcal{C}_\alpha^{\text{PP}}) \geq 1 - \alpha.$$

For example, if the loss $\ell_\theta(x, y)$ takes values in $[0, B]$ for all x, y , then we can set $\mathcal{T}_{\alpha-\delta}(\theta) = B\sqrt{\frac{\log(1/(\alpha-\delta))}{N}}$. The validity of this choice follows by Hoeffding's inequality.

Mode estimation. A commonplace inference task that does not fall under convex estimation is the problem of estimating the mode of the outcome distribution. When the outcome takes values in a discrete set Θ , this can be done by using the loss function $\ell_\theta(y) = \mathbb{1}\{y \neq \theta\}$, $\theta \in \Theta$. A generalization of this approach to continuous outcome distributions is obtained by defining the loss $\ell_\theta(y) = \mathbb{1}\{|y - \theta| > \eta\}$, for some width parameter $\eta > 0$. The target of inference is thus the point $\theta \in \mathbb{R}$ that has the most probability mass in its η -neighborhood, $\theta^* = \arg \min_{\theta \in \mathbb{R}} P(|Y_1 - \theta| > \eta)$. Theorem 2 applies directly in both the discrete and continuous cases.

Tukey's biweight robust mean. The Tukey biweight loss function is a commonly used loss in robust statistics that results in an outlier-robust mean estimate. It behaves approximately like a quadratic near the origin and is constant far away from the origin. Formally, Tukey's biweight loss function is given by

$$\ell_\theta(y) = \begin{cases} \frac{c^2}{6} \left(1 - \left(1 - \frac{(y-\theta)^2}{c^2} \right)^3 \right), & |y - \theta| \leq c, \\ \frac{c^2}{6}, & \text{otherwise,} \end{cases}$$

where c is a user-specified tuning parameter. It is not hard to see that the function $\ell_\theta(y)$ is nonconvex and hence not amenable to the analysis in Section 2; however, Theorem 2 applies.

Model selection. Nonconvex risk minimization problems are ubiquitous in model selection. For example, a common model selection strategy is best subset selection, which optimizes the squared loss, $\ell_\theta(x, y) = (y - x^\top \theta)^2$, subject to the constraint $\Theta = \{\theta \in \mathbb{R}^d : \|\theta\|_0 \leq k\}$. Here, Θ is the space of all k -sparse vectors for a user-chosen parameter k . Even though the loss function is convex, Θ is a nonconvex constraint set and hence we cannot rely on the condition (1) to find the minimizer. However, Theorem 2 still applies.

4.2 Inference under distribution shift

In Section 2 we focused on forming prediction-powered confidence intervals when the labeled and unlabeled data come from the same distribution. Herein, we extend our tools to the case where the labeled data (X, Y) comes from \mathbb{P} and the unlabeled data (\tilde{X}, \tilde{Y}) —which defines the target of inference θ^* —comes from \mathbb{Q} , and these are related by either a label shift or a covariate shift. For covariate shift, we handle all estimation problems previously studied; for label shift, we handle certain types of linear problems.

We will write $\mathbb{E}_\mathbb{Q}, \mathbb{E}_\mathbb{P}$, etc to indicate which distribution the data inside the expectation is sampled from.

4.2.1 Covariate shift

First, we assume that \mathbb{Q} is a known *covariate shift* of \mathbb{P} . That is, if we denote by $\mathbb{Q} = \mathbb{Q}_X \cdot \mathbb{Q}_{Y|X}$ and $\mathbb{P} = \mathbb{P}_X \cdot \mathbb{P}_{Y|X}$ the relevant marginal and conditional distributions, we assume that $\mathbb{Q}_{Y|X} = \mathbb{P}_{Y|X}$. As in previous sections, we consider estimands of the form

$$\theta^* = \arg \min_{\theta \in \Theta} \mathbb{E}_\mathbb{Q}[\ell_\theta(X_1, Y_1)]. \quad (10)$$

Estimands of the form (10) can be related to risk minimizers on \mathbb{P} using the Radon-Nikodym derivative. In particular, suppose that \mathbb{Q}_X is dominated by \mathbb{P}_X and assume that the Radon-Nikodym derivative $w(x) = \frac{\mathbb{Q}_X}{\mathbb{P}_X}(x)$ is known. Then, we can rewrite (10) as

$$\theta^* = \arg \min_{\theta \in \Theta} \mathbb{E}_{\mathbb{P}}[\ell_{\theta}^w(X_1, Y_1)],$$

where $\ell_{\theta}^w(x, y) = w(x)\ell_{\theta}(x, y)$. In words, risk minimizers on \mathbb{Q} can simply be written as risk minimizers on \mathbb{P} , but with a reweighted loss function. This permits inference on the rectifier to be based on data sampled from \mathbb{P} as before. For concreteness, we explain the approach in detail for convex risk minimizers. Let

$$\Delta^{f,w}(\theta) = \mathbb{E}_{\mathbb{P}}[g_{\theta}^w(X_1, Y_1) - g_{\theta}^w(X_1, f_1)],$$

where $g_{\theta}^w(x, y) = g_{\theta}(x, y) \cdot w(x)$ and g_{θ} is a subgradient of ℓ_{θ} as before. A confidence set for the above rectifier suffices for prediction-powered inference on θ^* .

Corollary 1 (Covariate shift). *Suppose that the problem (10) is a nondegenerate convex estimation problem. Fix $\alpha \in (0, 1)$ and $\delta \in (0, \alpha)$. Suppose that, for any $\theta \in \mathbb{R}^p$, we can construct $\mathcal{R}_{\delta}(\theta)$ and $\mathcal{T}_{\alpha-\delta}(\theta)$ satisfying*

$$P(\Delta^{f,w}(\theta) \in \mathcal{R}_{\delta}(\theta)) \geq 1 - \delta; \quad P(\mathbb{E}[g_{\theta}^w(X_1, f_1)] \in \mathcal{T}_{\alpha-\delta}(\theta)) \geq 1 - (\alpha - \delta).$$

Let $\mathcal{C}_{\alpha}^{\text{PP}} = \{\theta : 0 \in \mathcal{R}_{\delta}(\theta) + \mathcal{T}_{\alpha-\delta}(\theta)\}$, where $+$ denotes the Minkowski sum. Then,

$$P(\theta^* \in \mathcal{C}_{\alpha}^{\text{PP}}) \geq 1 - \alpha.$$

The same reweighting principle can be used to handle nonconvex risk minimizers as in Section 4.1.

4.2.2 Label shift

Next, we analyze classification problems where the proportions of the classes in the labeled data is different from those in the unlabeled data. Formally, let $\mathcal{Y} = \{1, \dots, K\}$ be the label space and assume that $\mathbb{Q}_{X|Y} = \mathbb{P}_{X|Y}$. We consider estimands of the form

$$\theta^* = \mathbb{E}_{\mathbb{Q}_Y}[\nu(Y)],$$

where $\nu : \mathcal{Y} \rightarrow \mathbb{R}$ is a fixed function. For example, choosing $\nu(y) = \mathbb{1}\{y = k\}$ for some $k \in [K]$ asks for inference on the proportion of instances that belong to class k .

Using an analogous decomposition to the one for mean estimation, we can write

$$\theta^* = \mathbb{E}_{\mathbb{Q}_f}[\nu(f)] + (\mathbb{E}_{\mathbb{Q}_Y}[\nu(Y)] - \mathbb{E}_{\mathbb{Q}_f}[\nu(f)]) = \theta^f + \Delta^f,$$

where \mathbb{Q}_f denotes the distribution of $f(X)$, $X \sim \mathbb{Q}_X$. The quantity θ^f can be estimated using the unlabeled data from \mathbb{Q} and the model. Estimating the quantity Δ^f using samples from \mathbb{P} will require leveraging the structure of the distribution shift. Central to our analysis will be the confusion matrix

$$\mathcal{K}_{j,l} = \mathbb{Q}(f(X) = j \mid Y = l), \quad j, l \in [K].$$

The label-shift assumption implies that $\mathcal{K}_{j,l} = \mathbb{P}(f(X) = j \mid Y = l)$, which can be estimated from labeled data sampled from \mathbb{P} . In particular, we estimate \mathcal{K} from the labeled data as

$$\hat{\mathcal{K}}_{j,l} = \frac{1}{n(l)} \sum_{i=1}^n \mathbb{1}\{f_i = j, Y_i = l\}, \quad \text{where } n(l) = \sum_{i=1}^n \mathbb{1}\{Y_i = l\}.$$

Similarly, we can estimate $\mathbb{Q}_f(k)$, $k \in [K]$ as

$$\hat{\mathbb{Q}}_f(k) = \frac{1}{N} \sum_{i=1}^N \mathbb{1}\{\tilde{f}_i = k\}.$$

Treating \mathbb{Q}_f and \mathbb{Q}_Y as vectors, notice that we can write $\mathbb{Q}_f = \mathcal{K}\mathbb{Q}_Y$, and hence $\mathbb{Q}_Y = \mathcal{K}^{-1}\mathbb{Q}_f$. This leads to a natural estimate of \mathbb{Q}_Y , $\hat{\mathbb{Q}}_Y = \hat{\mathcal{K}}^{-1}\hat{\mathbb{Q}}_f$. Below, we use these quantities to construct a prediction-powered confidence interval for $\theta^* = \mathbb{E}_{\mathbb{Q}_Y}[\nu(Y)]$.

Theorem 3 (Label shift). *Fix $\alpha \in (0, 1)$ and $\delta \in (0, \alpha)$. Let*

$$\mathcal{C}_\alpha^{\text{PP}} = \left(\mathbb{E}_{\hat{\mathbb{Q}}_Y}[\nu(Y)] \pm \left(\max_{l, k \in [K]} \max_{p \in C_{l,k}} |\hat{\mathcal{K}}_{l,k} - p| + \sqrt{\frac{1}{2N} \log \frac{2}{\alpha - \delta}} \right) \right),$$

where

$$C_{l,k} = \left\{ p : n(k) \hat{\mathcal{K}}_{l,k} \in \left[F_{\text{Binom}(n(k), p)}^{-1} \left(\frac{\delta}{2K^2} \right), F_{\text{Binom}(n(k), p)}^{-1} \left(1 - \frac{\delta}{2K^2} \right) \right] \right\}$$

and $F_{\text{Binom}(n(k), p)}$ denotes the Binomial CDF. Then,

$$P(\theta^* \in \mathcal{C}_\alpha^{\text{PP}}) \geq 1 - \alpha.$$

Naturally, the confidence interval becomes more conservative as the number of classes grows. Also, the power of the bound depends on the smallest number of instances observed for a particular class.

5 Acknowledgments

We would like to thank Amit Kohli for suggesting the term “rectifier,” Eric Orenstein for helpful discussions related to the WHO-I Plankton data set, Philip Stark and the San Francisco Department of Elections for helping us find the ballot data set, and Sherrie Wang for help with the remote sensing experiment. This work was supported in part by the Mathematical Data Science program of the Office of Naval Research under grant number N00014-21-1-2840 and the National Science Foundation Graduate Research Fellowship.

References

- [1] J. Jumper, R. Evans, A. Pritzel, T. Green, M. Figurnov, O. Ronneberger, K. Tunyasuvunakool, R. Bates, A. Židek, A. Potapenko, *et al.*, “Highly accurate protein structure prediction with AlphaFold,” *Nature*, vol. 596, no. 7873, pp. 583–589, 2021.
- [2] E. L. Bullock, C. E. Woodcock, C. Souza Jr, and P. Olofsson, “Satellite-based estimates reveal widespread forest degradation in the Amazon,” *Global Change Biology*, vol. 26, no. 5, pp. 2956–2969, 2020.
- [3] J. O. Sexton, X.-P. Song, M. Feng, P. Noojipady, A. Anand, C. Huang, D.-H. Kim, K. M. Collins, S. Channan, C. DiMiceli, *et al.*, “Global, 30-m resolution continuous fields of tree cover: Landsat-based rescaling of modis vegetation continuous fields with lidar-based estimates of error,” *International Journal of Digital Earth*, vol. 6, no. 5, pp. 427–448, 2013.
- [4] I. Bludau, S. Willems, W.-F. Zeng, M. T. Strauss, F. M. Hansen, M. C. Tanzer, O. Karayel, B. A. Schulman, and M. Mann, “The structural context of posttranslational modifications at a proteome-wide scale,” *PLoS Biology*, vol. 20, no. 5, e3001636, 2022.
- [5] X. J. Zhu, “Semi-supervised learning literature survey,” 2005.
- [6] P. J. Huber, “Under nonstandard conditions,” in *Proceedings of the Fifth Berkeley Symposium on Mathematical Statistics and Probability: Weather Modification; University of California Press: Berkeley, CA, USA*, 1967, p. 221.
- [7] H. White, “A heteroskedasticity-consistent covariance matrix estimator and a direct test for heteroskedasticity,” *Econometrica: Journal of the Econometric Society*, pp. 817–838, 1980.
- [8] K.-Y. Liang and S. L. Zeger, “Longitudinal data analysis using generalized linear models,” *Biometrika*, vol. 73, no. 1, pp. 13–22, 1986.
- [9] A. Buja, L. Brown, R. Berk, E. George, E. Pitkin, M. Traskin, K. Zhang, and L. Zhao, “Models as approximations I: Consequences illustrated with linear regression,” *Statistical Science*, vol. 34, no. 4, pp. 523–544, 2019.

- [10] C.-E. Särndal, B. Swensson, and J. Wretman, *Model Assisted Survey Sampling*. Springer Science & Business Media, 1992.
- [11] C. M. Cassel, C. E. Särndal, and J. H. Wretman, “Some results on generalized difference estimation and generalized regression estimation for finite populations,” *Biometrika*, vol. 63, no. 3, pp. 615–620, 1976.
- [12] C. Wu and R. R. Sitter, “A model-calibration approach to using complete auxiliary information from survey data,” *Journal of the American Statistical Association*, vol. 96, no. 453, pp. 185–193, 2001.
- [13] F. J. Breidt and J. D. Opsomer, “Model-assisted survey estimation with modern prediction techniques,” *Statistical Science*, vol. 32, no. 2, pp. 190–205, 2017.
- [14] X. Zhu and A. B. Goldberg, “Introduction to semi-supervised learning,” *Synthesis Lectures on Artificial Intelligence and Machine Learning*, vol. 3, no. 1, pp. 1–130, 2009.
- [15] R. J. Little and D. B. Rubin, *Statistical Analysis with Missing Data*. John Wiley & Sons, 2019, vol. 793.
- [16] S. Wang, T. H. McCormick, and J. T. Leek, “Methods for correcting inference based on outcomes predicted by machine learning,” *Proceedings of the National Academy of Sciences*, vol. 117, no. 48, pp. 30 266–30 275, 2020.
- [17] R. Koenker and G. Bassett Jr, “Regression quantiles,” *Econometrica: Journal of the Econometric Society*, pp. 33–50, 1978.
- [18] B. Efron, *Exponential Families in Theory and Practice*. Cambridge University Press, 2022.
- [19] D. Desilver, “On Election Day, most voters use electronic or optical-scan ballots,” *Fact Tank*, 2016.
- [20] M. Lindeman and P. B. Stark, “A gentle introduction to risk-limiting audits,” *IEEE Security & Privacy*, vol. 10, no. 5, pp. 42–49, 2012.
- [21] F. Ding, M. Hardt, J. Miller, and L. Schmidt, “Retiring adult: New datasets for fair machine learning,” *Advances in Neural Information Processing Systems*, vol. 34, pp. 6478–6490, 2021.
- [22] T. Chen and C. Guestrin, “Xgboost: A scalable tree boosting system,” in *Proceedings of the 22nd ACM SIGKDD International Conference on Knowledge Discovery and Data Mining*, 2016, pp. 785–794.
- [23] E. D. Vaishnav, C. G. de Boer, J. Molinet, M. Yassour, L. Fan, X. Adiconis, D. A. Thompson, J. Z. Levin, F. A. Cubillos, and A. Regev, “The evolution, evolvability and engineering of gene regulatory DNA,” *Nature*, vol. 603, no. 7901, pp. 455–463, Mar. 2022.
- [24] R. J. Olson, A. Shalapyonok, and H. M. Sosik, “An automated submersible flow cytometer for analyzing pico-and nanophytoplankton: Flowcytobot,” *Deep Sea Research Part I: Oceanographic Research Papers*, vol. 50, no. 2, pp. 301–315, 2003.
- [25] E. C. Orenstein, O. Beijbom, E. E. Peacock, and H. M. Sosik, “WhoI-plankton-a large scale fine grained visual recognition benchmark dataset for plankton classification,” *arXiv preprint arXiv:1510.00745*, 2015.
- [26] K. He, X. Zhang, S. Ren, and J. Sun, “Deep residual learning for image recognition,” in *Proceedings of the IEEE Conference on Computer Vision and Pattern Recognition (CVPR)*, 2016, pp. 770–778.
- [27] I. Waudby-Smith and A. Ramdas, “Estimating means of bounded random variables by betting,” *arXiv preprint arXiv:2010.09686*, 2020.
- [28] H. White, “Using least squares to approximate unknown regression functions,” *International Economic Review*, pp. 149–170, 1980.
- [29] A. Dvoretzky, J. Kiefer, and J. Wolfowitz, “Asymptotic minimax character of the sample distribution function and of the classical multinomial estimator,” *The Annals of Mathematical Statistics*, pp. 642–669, 1956.
- [30] P. Massart, “The tight constant in the Dvoretzky-Kiefer-Wolfowitz inequality,” *The Annals of Probability*, pp. 1269–1283, 1990.
- [31] C. L. Canonne, “A short note on learning discrete distributions,” *arXiv preprint arXiv:2002.11457*, 2020.

- [32] P. Erdős, “On the central limit theorem for samples from a finite population,” *Publications of the Mathematical Institute of the Hungarian Academy of Sciences*, vol. 4, pp. 49–61, 1959.
- [33] T. Höglund, “Sampling from a finite population. A remainder term estimate,” *Scandinavian Journal of Statistics*, pp. 69–71, 1978.

A Inference on a finite population

The techniques developed in this paper directly translate to the *finite-population* setting. Here, we treat (\tilde{X}, \tilde{Y}) as a fixed finite population consisting of N feature-outcome pairs, without imposing any distributional assumptions on the data points. Analogously to the i.i.d. setting, we observe all features \tilde{X} and a small set of outcomes. Specifically, we assume that we observe $(\tilde{Y}_i)_{i \in \mathcal{I}}$, where $\mathcal{I} = \{i_1, \dots, i_n\}$ is a uniformly sampled subset of $[N]$ of size $n \ll N$. In this section we adapt all our main results to the finite-population context.

Given a loss function ℓ_θ and parameter space Θ , the target estimand is the risk minimizer we would compute if we could observe the whole population:

$$\theta^* = \arg \min_{\theta \in \Theta} \frac{1}{N} \sum_{i=1}^N \ell_\theta(\tilde{X}_i, \tilde{Y}_i). \quad (11)$$

The following two subsections mirror the results for convex and nonconvex estimation from the main body of the paper. All results in this section are proved essentially identically as their i.i.d. counterparts.

In what follows, we construct prediction-powered confidence sets $\mathcal{C}_\alpha^{\text{PP}}$ assuming a valid confidence set around the rectifier (defined below for the finite-population context). The confidence set for the rectifier can be constructed from $(\tilde{X}_i, \tilde{Y}_i)_{i \in \mathcal{I}}$ via a direct application of off-the-shelf results outlined in Appendix D. In particular, in Proposition D.4 we state an asymptotically valid interval for the mean based on a finite-population version of the central limit theorem, and in Proposition D.3 we state a nonasymptotically valid interval for the mean for finite populations due to Waudby-Smith and Ramdas [27]. The only assumption required to apply the latter is that $g_\theta(\tilde{X}_i, \tilde{Y}_i) - g_\theta(\tilde{X}_i, \tilde{f}_i)$ has a known bound valid for all $i \in [N]$.

A.1 Convex estimation

In the finite-population setting, the mild nondegeneracy condition ensured by convexity takes the form

$$\frac{1}{N} \sum_{i=1}^N g_{\theta^*}(\tilde{X}_i, \tilde{Y}_i) = 0, \quad (12)$$

where g_θ is a subgradient of ℓ_θ . The rectifier is thus:

$$\Delta^f(\theta) = \frac{1}{N} \sum_{i=1}^N \left(g_\theta(\tilde{X}_i, \tilde{Y}_i) - g_\theta(\tilde{X}_i, \tilde{f}_i) \right).$$

Theorem A.1 (Convex estimation, finite population). *Suppose that the convex estimation problem is non-degenerate (12). Fix $\alpha \in (0, 1)$. Suppose that, for any $\theta \in \mathbb{R}^p$, we can construct $\mathcal{R}_\alpha(\theta)$ satisfying*

$$P(\Delta^f(\theta) \in \mathcal{R}_\alpha(\theta)) \geq 1 - \alpha.$$

Let $\mathcal{C}_\alpha^{\text{PP}} = \left\{ \theta : -\frac{1}{N} \sum_{i=1}^N g_\theta(\tilde{X}_i, \tilde{f}_i) \in \mathcal{R}_\alpha(\theta) \right\}$. Then,

$$P(\theta^* \in \mathcal{C}_\alpha^{\text{PP}}) \geq 1 - \alpha.$$

We apply Theorem A.1 in the context of mean estimation, quantile estimation, logistic regression, and linear regression. The target estimand θ^* is defined as in (11) with the loss function chosen appropriately, as discussed in Section 2.1. We remark that, just like in the i.i.d. case, the analysis for linear regression follows a more refined approach, as in the proof of Proposition 4.

Corollary A.1 (Mean estimation, finite population). *Let θ^* be the mean outcome. Fix $\alpha \in (0, 1)$. Suppose that, for any $\theta \in \mathbb{R}$, we can construct an interval $(\mathcal{R}_\alpha^l, \mathcal{R}_\alpha^u)$ such that $P(\Delta^f \in (\mathcal{R}_\alpha^l, \mathcal{R}_\alpha^u)) \geq 1 - \alpha$, where*

$$\Delta^f = \frac{1}{N} \sum_{i=1}^N (\tilde{f}_i - \tilde{Y}_i).$$

Let

$$\mathcal{C}_\alpha^{\text{PP}} = \left(\frac{1}{N} \sum_{i=1}^N \tilde{f}_i - \mathcal{R}_\alpha^u, \frac{1}{N} \sum_{i=1}^N \tilde{f}_i - \mathcal{R}_\alpha^l \right).$$

Then,

$$P(\theta^* \in \mathcal{C}_\alpha^{\text{PP}}) \geq 1 - \alpha.$$

Corollary A.2 (Quantile estimation, finite population). *Let θ^* be the q -quantile. Fix $\alpha \in (0, 1)$. Suppose that, for any $\theta \in \mathbb{R}$, we can construct an interval $(\mathcal{R}_\alpha^l(\theta), \mathcal{R}_\alpha^u(\theta))$ such that $P(\Delta^f(\theta) \in (\mathcal{R}_\alpha^l(\theta), \mathcal{R}_\alpha^u(\theta))) \geq 1 - \alpha$, where*

$$\Delta^f(\theta) = \frac{1}{N} \sum_{i=1}^N \left(\mathbb{1}\{\tilde{f}_i \leq \theta\} - \mathbb{1}\{\tilde{Y}_i \leq \theta\} \right).$$

Let

$$\mathcal{C}_\alpha^{\text{PP}} = \left\{ \theta \in \mathbb{R} : \frac{1}{N} \sum_{i=1}^N \mathbb{1}\{\tilde{f}_i \leq \theta\} \in (q + \mathcal{R}_\alpha^l(\theta), q + \mathcal{R}_\alpha^u(\theta)) \right\}.$$

Then,

$$P(\theta^* \in \mathcal{C}_\alpha^{\text{PP}}) \geq 1 - \alpha.$$

Corollary A.3 (Logistic regression, finite population). *Let θ^* be the logistic regression solution. Fix $\alpha \in (0, 1)$. Suppose that we can construct $\mathcal{R}_\alpha^l, \mathcal{R}_\alpha^u \in \mathbb{R}^d$ such that $P(\Delta_j^f \in (\mathcal{R}_{\alpha,j}^l, \mathcal{R}_{\alpha,j}^u), \forall j \in [d]) \geq 1 - \alpha$, where*

$$\Delta^f = \frac{1}{N} \sum_{i=1}^N \tilde{X}_i(\tilde{f}_i - \tilde{Y}_i).$$

Let

$$\mathcal{C}_\alpha^{\text{PP}} = \left\{ \theta \in \mathbb{R}^d : \frac{1}{N} \sum_{i=1}^N \tilde{X}_{i,j} \left(\tilde{f}_i - \frac{1}{1 + \exp(-\tilde{X}_i^\top \theta)} \right) \in (\mathcal{R}_{\alpha,j}^l, \mathcal{R}_{\alpha,j}^u), \forall j \in [d] \right\}.$$

Then,

$$P(\theta^* \in \mathcal{C}_\alpha^{\text{PP}}) \geq 1 - \alpha.$$

Corollary A.4 (Linear regression, finite population). *Let θ^* be the linear regression solution. Fix $\alpha \in (0, 1)$. Suppose that we can construct $\mathcal{R}_\alpha^l, \mathcal{R}_\alpha^u \in \mathbb{R}^d$ such that $P(\Delta_j^f \in (\mathcal{R}_{\alpha,j}^l, \mathcal{R}_{\alpha,j}^u), \forall j \in [d]) \geq 1 - \alpha$, where*

$$\Delta^f = \tilde{X}^\dagger(\tilde{f} - \tilde{Y}).$$

Let

$$\mathcal{C}_\alpha^{\text{PP}} = \left(\tilde{X}^\dagger \tilde{f} - \mathcal{R}_\alpha^u, \tilde{X}^\dagger \tilde{f} - \mathcal{R}_\alpha^l \right).$$

Then,

$$P(\theta^* \in \mathcal{C}_\alpha^{\text{PP}}) \geq 1 - \alpha.$$

A.2 Beyond convex estimation

We now consider general risk minimizers in the finite-population context. The rectifier is equal to:

$$\Delta^f(\theta) = \frac{1}{N} \sum_{i=1}^N \left(\ell_\theta(\tilde{X}_i, \tilde{Y}_i) - \ell_\theta(\tilde{X}_i, \tilde{f}_i) \right).$$

Unlike in the i.i.d. setting, there is no need for data splitting because the imputed estimate is deterministic. We let:

$$\tilde{L}^f(\theta) := \frac{1}{N} \sum_{i=1}^N \ell_\theta(\tilde{X}_i, \tilde{f}_i); \quad \tilde{\theta}^f = \arg \min_{\theta \in \Theta} \tilde{L}^f(\theta).$$

Theorem A.2 (General risk minimization, finite population). *Fix $\alpha \in (0, 1)$. Suppose that, for any $\theta \in \Theta$, we can construct $(\mathcal{R}_{\alpha/2}^l(\theta), \mathcal{R}_{\alpha/2}^u(\theta))$ such that*

$$P\left(\Delta^f(\theta) \leq \mathcal{R}_{\alpha/2}^u(\theta)\right) \geq 1 - \alpha/2; \quad P\left(\Delta^f(\theta) \geq \mathcal{R}_{\alpha/2}^l(\theta)\right) \geq 1 - \alpha/2.$$

Let

$$\mathcal{C}_\alpha^{\text{PP}} = \left\{ \theta \in \Theta : \tilde{L}^f(\theta) \leq \tilde{L}^f(\tilde{\theta}^f) - \mathcal{R}_{\alpha/2}^l(\theta) + \mathcal{R}_{\alpha/2}^u(\tilde{\theta}^f) \right\}.$$

Then, we have

$$P(\theta^* \in \mathcal{C}_\alpha^{\text{PP}}) \geq 1 - \alpha.$$

B Deferred theoretical details

We state an asymptotic counterpart of Theorem 1 that is used to prove the propositions in Section 2.1. Then, we provide nonasymptotically-valid counterparts of the algorithms in Section 2.1. Finally, we state the regularity conditions necessary for the guarantees presented in Section 2.1.

B.1 Asymptotic counterpart of Theorem 1

The following is an asymptotic counterpart of Theorem 1 that uses the central limit theorem in the confidence set construction. We note the error budget splitting used in Theorem 1 is in fact not necessary, but we believe that it facilitates exposition when presenting nonasymptotic guarantees. The asymptotic result below is stated without the splitting of the error budget. The proof is stated in Appendix C.

Theorem B.1 (Convex estimation: asymptotic version). *Suppose that the convex estimation problem is nondegenerate as in (1) and that $\frac{n}{N} \rightarrow p$, for some $p \in (0, 1)$. Fix $\alpha \in (0, 1)$. For all $\theta \in \mathbb{R}^p$, define*

$$\hat{\Delta}^f(\theta) = \frac{1}{n} \sum_{i=1}^n (g_\theta(X_i, Y_i) - g_\theta(X_i, f_i)); \quad \hat{g}^f(\theta) = \frac{1}{N} \sum_{i=1}^N g_\theta(\tilde{X}_i, \tilde{f}_i).$$

Further, denoting by $g_{\theta,j}(x, y)$ the j -th coordinate of $g_\theta(x, y)$, let

$$\hat{\sigma}_{\Delta,j}^2(\theta) = \frac{1}{n} \sum_{i=1}^n \left(g_{\theta,j}(X_i, Y_i) - g_{\theta,j}(X_i, f_i) - \hat{\Delta}_j^f(\theta) \right)^2; \quad \hat{\sigma}_{g,j}^2(\theta) = \frac{1}{N} \sum_{i=1}^N \left(g_{\theta,j}(\tilde{X}_i, \tilde{f}_i) - \hat{g}_j^f(\theta) \right)^2,$$

for all $j \in [p]$. Let $w_{\alpha,j}(\theta) = z_{1-\alpha/(2p)} \sqrt{\frac{\hat{\sigma}_{\Delta,j}^2(\theta)}{n} + \frac{\hat{\sigma}_{g,j}^2(\theta)}{N}}$ and $\mathcal{C}_\alpha^{\text{PP}} = \left\{ \theta : |\hat{\Delta}_j^f(\theta) + \hat{g}_j^f(\theta)| \leq w_{\alpha,j}(\theta), \forall j \in [p] \right\}$.

Then,

$$\liminf_{n, N \rightarrow \infty} P(\theta^* \in \mathcal{C}_\alpha^{\text{PP}}) \geq 1 - \alpha.$$

B.2 Algorithms with nonasymptotic validity

We state nonasymptotically-valid algorithms for prediction-powered mean estimation, quantile estimation, and logistic regression. Like the methods in Section 2.1, the algorithms rely on the abstract recipe from Theorem 1. The proofs of validity are included in Appendix C.

The following results all construct a prediction-powered confidence set $\mathcal{C}_\alpha^{\text{PP}}$, assuming a valid confidence set around the rectifier (defined for each result individually). We do not write out the confidence set for the rectifier explicitly for clarity, but it can be constructed via a direct application of Proposition D.1. Proposition D.1 states a nonasymptotic, variance-adaptive confidence interval for the mean due to Waudby-Smith and Ramdas [27]. We opt to present this construction as the default nonasymptotic confidence interval for the mean because of its strong practical performance. The only assumption required to apply Proposition D.1 and form a set around $\Delta^f(\theta)$ is that $g_\theta(X_1, Y_1) - g_\theta(X_1, f_1)$ is almost surely bounded.

Corollary B.1 (Mean estimation). *Let θ^* be the mean outcome (3). Fix $\alpha \in (0, 1)$ and $\delta \in (0, \alpha)$. Assume that $|f_1| \leq B$ almost surely. Suppose that we can construct an interval $(\mathcal{R}_\delta^l, \mathcal{R}_\delta^u)$ such that $P(\Delta^f \in (\mathcal{R}_\delta^l, \mathcal{R}_\delta^u)) \geq 1 - \delta$, where $\Delta^f = \mathbb{E}[f_1 - Y_1]$. Let*

$$\mathcal{C}_\alpha^{\text{PP}} = \left(\frac{1}{N} \sum_{i=1}^N \tilde{f}_i - \mathcal{R}_\delta^u - B \sqrt{\frac{2 \log(\frac{2}{\alpha-\delta})}{N}}, \frac{1}{N} \sum_{i=1}^N \tilde{f}_i - \mathcal{R}_\delta^l + B \sqrt{\frac{2 \log(\frac{2}{\alpha-\delta})}{N}} \right).$$

Then,

$$P(\theta^* \in \mathcal{C}_\alpha^{\text{PP}}) \geq 1 - \alpha.$$

Corollary B.2 (Quantile estimation). *Let θ^* be the q -quantile (4). Fix $\alpha \in (0, 1)$ and $\delta \in (0, \alpha)$. Suppose that, for any $\theta \in \mathbb{R}$, we can construct an interval $(\mathcal{R}_\delta^l(\theta), \mathcal{R}_\delta^u(\theta))$ such that $P(\Delta^f(\theta) \in (\mathcal{R}_\delta^l(\theta), \mathcal{R}_\delta^u(\theta))) \geq 1 - \delta$, where $\Delta^f(\theta) = \mathbb{E}[\mathbb{1}\{f_1 \leq \theta\} - \mathbb{1}\{Y_1 \leq \theta\}]$. Let*

$$\mathcal{C}_\alpha^{\text{PP}} = \left\{ \theta \in \mathbb{R} : \frac{1}{N} \sum_{i=1}^N \mathbb{1}\{\tilde{f}_i \leq \theta\} \in \left(q + \mathcal{R}_\delta^l(\theta) - \sqrt{\frac{\log(\frac{2}{\alpha-\delta})}{2N}}, q + \mathcal{R}_\delta^u(\theta) + \sqrt{\frac{\log(\frac{2}{\alpha-\delta})}{2N}} \right) \right\}.$$

Then,

$$P(\theta^* \in \mathcal{C}_\alpha^{\text{PP}}) \geq 1 - \alpha.$$

Corollary B.3 (Logistic regression). *Let θ^* be the logistic regression solution (5). Fix $\alpha \in (0, 1)$ and $\delta \in (0, \alpha)$. Suppose $|X_{1,i}| \leq B_i, i \in [d]$ and $Y_1 \in [0, 1]$ almost surely, and suppose that we can construct $\mathcal{R}_\delta^l, \mathcal{R}_\delta^u \in \mathbb{R}^d$ such that $P(\Delta_j^f \in (\mathcal{R}_{\delta,j}^l, \mathcal{R}_{\delta,j}^u), \forall j \in [d]) \geq 1 - \delta$, where $\Delta^f = \mathbb{E}[X_1(f_1 - Y_1)]$. Let*

$$\mathcal{C}_\alpha^{\text{PP}} = \left\{ \theta \in \mathbb{R}^d : \frac{1}{N} \sum_{i=1}^N \tilde{X}_{i,j} (\tilde{f}_i - \mu_\theta(\tilde{X}_i)) \in \left(\mathcal{R}_{\delta,j}^l - B_j \sqrt{\frac{8 \log(\frac{2d}{\alpha-\delta})}{N}}, \mathcal{R}_{\delta,j}^u + B_j \sqrt{\frac{8 \log(\frac{2d}{\alpha-\delta})}{N}} \right), \forall j \in [d] \right\},$$

where $\mu_\theta(x) = 1/(1 + \exp(-x^\top \theta))$. Then,

$$P(\theta^* \in \mathcal{C}_\alpha^{\text{PP}}) \geq 1 - \alpha.$$

We note that there exists an analogous derivation for linear regression, however we do not recommend it in practice. The reason is that the refined (but asymptotic) analysis used to prove Proposition 4 shows that it is sufficient to analyze a one-dimensional rectifier, while directly invoking Theorem 1 would require analyzing a d -dimensional rectifier and thus yields more conservative intervals.

B.3 Regularity conditions

All algorithms stated in Section 2 rely on confidence intervals derived from the central limit theorem. For such intervals to be asymptotically valid, we require that the two quantities whose mean is being estimated, namely $g_\theta(X_1, Y_1) - g_\theta(X_1, f_1)$ and $g_\theta(X_1, f_1)$, have at least the first two moments (see Proposition D.2).

For Proposition 4 to hold, we need the same conditions as those required for classical linear regression intervals to cover the target. We note that these conditions are very weak; in particular, it is *not* required that the true data-generating process be linear or the errors be homoskedastic. See Buja, Brown, Berk, George, Pitkin, Traskin, Zhang, and Zhao [9] for a detailed discussion. The following are the required conditions, as stated in Theorem 3 of Halbert White's seminal paper [28]. The data $(X_1, Y_1), \dots, (X_n, Y_n)$ is generated as $X_i = h(Z_i)$, $Y_i = g(Z_i) + \epsilon_i$, where (Z_i, ϵ_i) are mean-zero i.i.d. random draws from some distribution such that $\mathbb{E}[Z_i Z_i^\top]$ and $\mathbb{E}[X_i X_i^\top]$ are finite and nonsingular, and $\mathbb{E}[\epsilon_i^2]$, $\mathbb{E}[Y_i^2 X_i X_i^\top]$, and $\mathbb{E}[X_{ij}^2 X_i X_i^\top]$ are all finite. In addition, we assume that h and g are measurable. Under these conditions,

$$\sqrt{n}(\hat{\theta}_{\text{OLS}} - \theta^*) \Rightarrow \mathcal{N}(0, \Sigma^{-1} V \Sigma^{-1}),$$

where $\theta^* = \arg \min_\theta \mathbb{E}[(Y_1 - X_1^\top \theta)^2]$, $\hat{\theta}_{\text{OLS}} = \arg \min_\theta \frac{1}{n} \sum_{i=1}^n (Y_i - X_i^\top \theta)^2$, $\Sigma = \mathbb{E}[X_1 X_1^\top]$, $V = \mathbb{E}[(Y_1 - X_1^\top \theta^*)^2 X_1 X_1^\top]$. Moreover, $\frac{1}{n} X^\top X \rightarrow \Sigma$ and $\frac{1}{n} \sum_{i=1}^n (Y_i - X_i^\top \hat{\theta}_{\text{OLS}})^2 X_i X_i^\top \rightarrow V$ almost surely.

C Proofs

C.1 Proof of Theorem 1

We show that $\theta^* \in \mathcal{C}_\alpha^{\text{PP}}$ with probability at least $1 - \alpha$; that is, with probability at least $1 - \alpha$ it holds that

$$0 \in \mathcal{R}_\delta(\theta^*) + \mathcal{T}_{\alpha-\delta}(\theta^*).$$

Consider the event $E = \{\Delta^f(\theta^*) \in \mathcal{R}_\delta(\theta^*)\} \cap \{\mathbb{E}[g_{\theta^*}(X_1, f_1)] \in \mathcal{T}_{\alpha-\delta}(\theta^*)\}$. By a union bound, $P(E) \geq 1 - \alpha$. On the event E , we have that

$$\begin{aligned} \mathbb{E}[g_{\theta^*}(X_1, Y_1)] &= \mathbb{E}[g_{\theta^*}(X_1, Y_1)] - \mathbb{E}[g_{\theta^*}(X_1, f_1)] + \mathbb{E}[g_{\theta^*}(X_1, f_1)] \\ &= \Delta^f(\theta^*) + \mathbb{E}[g_{\theta^*}(X_1, f_1)] \in \mathcal{R}_\delta(\theta^*) + \mathcal{T}_{\alpha-\delta}(\theta^*). \end{aligned}$$

The theorem finally follows by invoking the nondegeneracy condition, which ensures $\mathbb{E}[g_{\theta^*}(X_1, Y_1)] = 0$, so we have shown $0 \in \mathcal{R}_\delta(\theta^*) + \mathcal{T}_{\alpha-\delta}(\theta^*)$.

C.2 Proof of Theorem B.1

We show that $\theta^* \notin \mathcal{C}_\alpha^{\text{PP}}$ with probability at most α in the limit; that is,

$$\limsup_{n, N \rightarrow \infty} P \left(\left| \hat{\Delta}_j^f(\theta^*) + \hat{g}_j^f(\theta^*) \right| > z_{1-\alpha/(2p)} \sqrt{\frac{\hat{\sigma}_{\Delta,j}^2(\theta^*)}{n} + \frac{\hat{\sigma}_{g,j}^2(\theta^*)}{N}}, \forall j \in [p] \right) \leq \alpha.$$

For each $j \in [p]$, the central limit theorem implies that

$$\sqrt{n}(\hat{\Delta}_j^f(\theta^*) - \mathbb{E}[\hat{\Delta}_j^f(\theta^*)]) \Rightarrow \mathcal{N}(0, \sigma_{\Delta,j}^2(\theta^*)); \quad \sqrt{N}(\hat{g}_j^f(\theta^*) - \mathbb{E}[\hat{g}_j^f(\theta^*)]) \Rightarrow \mathcal{N}(0, \sigma_{g,j}^2(\theta^*)),$$

where $\sigma_{\Delta,j}^2(\theta^*)$ is the variance of $g_{\theta^*,j}(X_1, Y_1) - g_{\theta^*,j}(X_1, f_1)$ and $\sigma_{g,j}^2(\theta^*)$ is the variance of $g_{\theta^*,j}(X_1, f_1)$. Therefore, by Slutsky's theorem, we get

$$\begin{aligned} \sqrt{N}(\hat{\Delta}_j^f(\theta^*) + \hat{g}_j^f(\theta^*) - \mathbb{E}[\hat{\Delta}_j^f(\theta^*) + \hat{g}_j^f(\theta^*)]) &= \sqrt{n}(\hat{\Delta}_j^f(\theta^*) - \mathbb{E}[\hat{\Delta}_j^f(\theta^*)]) \sqrt{\frac{N}{n}} + \sqrt{N}(\hat{g}_j^f(\theta^*) - \mathbb{E}[\hat{g}_j^f(\theta^*)]) \\ &\Rightarrow \mathcal{N} \left(0, \frac{1}{p} \sigma_{\Delta,j}^2(\theta^*) + \sigma_{g,j}^2(\theta^*) \right). \end{aligned}$$

This in turn implies

$$\limsup_{n, N \rightarrow \infty} P \left(\left| \hat{\Delta}_j^f(\theta^*) + \hat{g}_j^f(\theta^*) - \mathbb{E}[\hat{\Delta}_j^f(\theta^*) + \hat{g}_j^f(\theta^*)] \right| > z_{1-\alpha/(2p)} \frac{\hat{\sigma}_j}{\sqrt{N}} \right) \leq \frac{\alpha}{p}, \quad (13)$$

where $\hat{\sigma}_j^2$ is a consistent estimate of the variance $\frac{1}{p} \sigma_{\Delta,j}^2(\theta^*) + \sigma_{g,j}^2(\theta^*)$. We take $\hat{\sigma}_j^2 = \hat{\sigma}_{\Delta,j}^2(\theta^*) \frac{N}{n} + \hat{\sigma}_{g,j}^2(\theta^*)$; this estimate is consistent since the two terms are individually consistent estimates of the respective variances. Now notice that

$$\mathbb{E}[\hat{\Delta}^f(\theta^*) + \hat{g}^f(\theta^*)] = \mathbb{E}[g_{\theta^*}(X_1, Y_1) - g_{\theta^*}(X_1, f_1) + g_{\theta^*}(\tilde{X}_1, \tilde{f}_1)] = \mathbb{E}[g_{\theta^*}(X_1, Y_1)] = 0, \quad (14)$$

where the last step follows by the nondegeneracy condition. Putting together (13), (14), and the choice of $\hat{\sigma}_j$ derived above, and applying a union bound, we get

$$\begin{aligned}
& \limsup_{n, N \rightarrow \infty} P \left(\exists j \in [p] : \left| \hat{\Delta}_j^f(\theta^*) + \hat{g}_j^f(\theta^*) \right| > z_{1-\alpha/(2p)} \sqrt{\frac{\hat{\sigma}_{\Delta,j}^2(\theta^*)}{n} + \frac{\hat{\sigma}_{g,j}^2(\theta^*)}{N}} \right) \\
& \leq \sum_{j=1}^p \limsup_{n, N \rightarrow \infty} P \left(\left| \hat{\Delta}_j^f(\theta^*) + \hat{g}_j^f(\theta^*) \right| > z_{1-\alpha/(2p)} \sqrt{\frac{\hat{\sigma}_{\Delta,j}^2(\theta^*)}{n} + \frac{\hat{\sigma}_{g,j}^2(\theta^*)}{N}} \right) \\
& = \sum_{j=1}^p \limsup_{n, N \rightarrow \infty} P \left(\left| \hat{\Delta}_j^f(\theta^*) + \hat{g}_j^f(\theta^*) - \mathbb{E} \left[\hat{\Delta}_j^f(\theta^*) + \hat{g}_j^f(\theta^*) \right] \right| > z_{1-\alpha/(2p)} \hat{\sigma}_j \right) \\
& \leq \sum_{j=1}^p \frac{\alpha}{p} \\
& = \alpha.
\end{aligned}$$

C.3 Proof of Proposition 1

We show that the prediction-powered confidence set constructed in Algorithm 1 is a special case of the prediction-powered confidence set constructed in Theorem B.1. The proof then follows directly by the guarantee of Theorem B.1.

Since $g_\theta(y) = \theta - y$, we have

$$\hat{\Delta}^f(\theta) \equiv \hat{\Delta}^f = \frac{1}{n} \sum_{i=1}^n (f_i - Y_i); \quad \hat{g}^f(\theta) = \theta - \frac{1}{N} \sum_{i=1}^N \tilde{f}_i.$$

Therefore, the set $\mathcal{C}_\alpha^{\text{PP}}$ from Theorem B.1 can be written as

$$\mathcal{C}_\alpha^{\text{PP}} = \left\{ \theta : \left| \theta - \frac{1}{N} \sum_{i=1}^N \tilde{f}_i + \frac{1}{n} \sum_{i=1}^n (f_i - Y_i) \right| \leq w_\alpha(\theta) \right\} = \left(\frac{1}{N} \sum_{i=1}^N \tilde{f}_i - \frac{1}{n} \sum_{i=1}^n (f_i - Y_i) \pm w_\alpha(\theta) \right).$$

This is exactly the set constructed in Algorithm 1, which completes the proof.

C.4 Proof of Proposition 2

Like in the proof of Proposition 1, we proceed by showing that the prediction-powered confidence set constructed in Algorithm 2 is a special case of the prediction-powered confidence set constructed in Theorem B.1. Then, we simply invoke Theorem B.1.

Since $g_\theta(y) = q - \mathbb{1}\{y \leq \theta\}$, we have

$$\hat{\Delta}^f(\theta) = \frac{1}{n} \sum_{i=1}^n (\mathbb{1}\{f_i \leq \theta\} - \mathbb{1}\{Y_i \leq \theta\}); \quad \hat{g}^f(\theta) = q - \hat{F}(\theta),$$

where $\hat{F}(\theta) = \frac{1}{N} \sum_{i=1}^N \mathbb{1}\{\tilde{f}_i \leq \theta\}$. Therefore, the set $\mathcal{C}_\alpha^{\text{PP}}$ from Theorem B.1 can be written as

$$\mathcal{C}_\alpha^{\text{PP}} = \left\{ \theta : \left| \frac{1}{n} \sum_{i=1}^n (\mathbb{1}\{f_i \leq \theta\} - \mathbb{1}\{Y_i \leq \theta\}) + q - \hat{F}(\theta) \right| \leq w_\alpha(\theta) \right\} = \left\{ \theta : \left| \hat{F}(\theta) - \hat{\Delta}^f(\theta) - q \right| \leq w_\alpha(\theta) \right\}.$$

This is exactly the set constructed in Algorithm 2. Therefore, the guarantee of Proposition 2 follows by the guarantee of Theorem B.1.

C.5 Proof of Proposition 3

The proof follows a similar pattern as the previous two propositions, by arguing that the prediction-powered confidence set constructed in Algorithm 3 is a special case of the prediction-powered confidence set constructed in Theorem B.1.

Since $g_\theta(x, y) = x(\mu_\theta(x) - y)$, we have

$$\hat{\Delta}^f(\theta) \equiv \hat{\Delta}^f = \frac{1}{n} \sum_{i=1}^n X_i(f_i - Y_i); \quad \hat{g}^f(\theta) = \frac{1}{N} \sum_{i=1}^N \tilde{X}_i(\mu_\theta(\tilde{X}_i) - \tilde{f}_i).$$

These quantities are explicitly computed in Algorithm 3. Moreover, the set $\mathcal{C}_\alpha^{\text{PP}}$ constructed in Algorithm 3 exactly follows the recipe of Theorem B.1, so the proof immediately follows.

C.6 Proof of Proposition 4

For linear regression, we can derive more powerful prediction-powered confidence intervals than those implied by Theorem 1 by exploiting the linearity of the least-squares estimator.

Recall that Theorem B.1 assumes that $\frac{n}{N} \rightarrow p$, for some fraction $p \in (0, 1)$.

Theorem 3 of White [7] implies that

$$\sqrt{n}(\hat{\Delta}^f - \Delta^f) \Rightarrow \mathcal{N}(0, W); \quad \sqrt{N}(\tilde{\theta}^f - \theta^f) \Rightarrow \mathcal{N}(0, W'),$$

for appropriately defined covariance matrices W and W' , where $\theta^f = (\mathbb{E}[X_1 X_1^\top])^{-1} \mathbb{E}[X_1 f_1]$ and $\Delta^f = (\mathbb{E}[X_1 X_1^\top])^{-1} \mathbb{E}[X_1(f_1 - Y_1)]$. With this, we can write the target estimand as $\theta^* = (\mathbb{E}[X_1 X_1^\top])^{-1} \mathbb{E}[X_1 Y_1] = \theta^f - \Delta^f$.

Combining Theorem 3 of White with Slutsky's theorem, we get

$$\sqrt{N}(\hat{\theta}^{\text{PP}} - \theta^*) = \sqrt{N}(\tilde{\theta}^f - \theta^f) - \sqrt{n}(\hat{\Delta}^f - \Delta^f) \sqrt{\frac{N}{n}} \Rightarrow \mathcal{N}\left(0, W \frac{1}{p} + W'\right).$$

White also shows that V and \tilde{V} , as defined in Algorithm 4, are consistent estimates of W and W' , respectively. Therefore, $\hat{\theta}^{\text{PP}}$ is asymptotically normal and consistent, and we have a consistent estimate of its covariance. In particular,

$$V_{j^*j^*} \frac{N}{n} + \tilde{V}_{j^*j^*} \rightarrow W_{j^*j^*} \frac{1}{p} + W'_{j^*j^*}.$$

This means that we can construct asymptotically valid confidence intervals via a normal approximation by choosing width $z_{1-\alpha/2} \sqrt{V_{j^*j^*} \frac{N}{n} + \tilde{V}_{j^*j^*} \frac{1}{N}} = z_{1-\alpha/2} \sqrt{\frac{V_{j^*j^*}}{n} + \frac{\tilde{V}_{j^*j^*}}{N}}$, and this is precisely what Algorithm 4 accomplishes.

C.7 Proof of Theorem 2

Define

$$L(\theta) = \mathbb{E}[\ell_\theta(X_1, Y_1)], \quad L^f(\theta) = \mathbb{E}[\ell_\theta(X_1, f_1)].$$

By the definition of θ^* , we have

$$\begin{aligned} \tilde{L}^f(\theta^*) &= (\tilde{L}^f(\theta^*) - L(\theta^*)) + (L(\theta^*) - L(\tilde{\theta}^f)) + (L(\tilde{\theta}^f) - \tilde{L}^f(\tilde{\theta}^f)) + \tilde{L}^f(\tilde{\theta}^f) \\ &\leq (\tilde{L}^f(\theta^*) - L(\theta^*)) + (L(\tilde{\theta}^f) - \tilde{L}^f(\tilde{\theta}^f)) + \tilde{L}^f(\tilde{\theta}^f). \end{aligned}$$

By applying the validity of the confidence bounds, a union bound implies that with probability $1 - \alpha$ we have

$$\begin{aligned}\tilde{L}^f(\theta^*) &\leq (L^f(\theta^*) - L(\theta^*)) + (L(\tilde{\theta}^f) - L^f(\tilde{\theta}^f)) + \tilde{L}^f(\tilde{\theta}^f) + \mathcal{T}_{\alpha-\delta}(\theta^*) \\ &= -\Delta^f(\theta^*) + \Delta^f(\tilde{\theta}^f) + \tilde{L}^f(\tilde{\theta}^f) + \mathcal{T}_{\alpha-\delta}(\theta^*) \\ &\leq -\mathcal{R}_{\delta/2}^l(\theta^*) + \mathcal{R}_{\delta/2}^u(\tilde{\theta}^f) + \tilde{L}^f(\tilde{\theta}^f) + \mathcal{T}_{\alpha-\delta}(\theta^*).\end{aligned}$$

Therefore, with probability $1 - \alpha$ we have that $\theta^* \in \mathcal{C}_\alpha^{\text{PP}}$, as desired.

C.8 Proof of Theorem 3

Notice that we can write $\mathbb{E}_{\mathbb{Q}_Y}[\nu(Y)] = \nu^\top \mathbb{Q}_Y$, where on the right-hand side we are treating $\nu = (\nu(1), \dots, \nu(K))$ and $\mathbb{Q}_Y = (\mathbb{Q}_Y(1), \dots, \mathbb{Q}_Y(K))$ as vectors of length K . We can write similar expressions for $\mathbb{Q}_f, \hat{\mathbb{Q}}_Y$, etc. Using this notation, by triangle inequality we have

$$|\theta^* - \nu^\top \hat{\mathbb{Q}}_Y| = |\nu^\top \mathbb{Q}_Y - \nu^\top \hat{\mathbb{Q}}_Y| \leq \left| \nu^\top \hat{\mathcal{K}}^{-1}(\mathbb{Q}_f - \hat{\mathbb{Q}}_f) \right| + \left| \nu^\top \mathcal{K}^{-1} \mathbb{Q}_f - \nu^\top \hat{\mathcal{K}}^{-1} \mathbb{Q}_f \right|. \quad (15)$$

We bound the first term using Hölder's inequality,

$$\left| \nu^\top \hat{\mathcal{K}}^{-1}(\mathbb{Q}_f - \hat{\mathbb{Q}}_f) \right| \leq \|\nu^\top \hat{\mathcal{K}}^{-1}\|_1 \|\mathbb{Q}_f - \hat{\mathbb{Q}}_f\|_\infty.$$

For the second term, we write

$$\left| \nu^\top \mathcal{K}^{-1} \mathbb{Q}_f - \nu^\top \hat{\mathcal{K}}^{-1} \mathbb{Q}_f \right| = \left| \nu^\top \hat{\mathcal{K}}^{-1}(\hat{\mathcal{K}} - \mathcal{K})\mathcal{K}^{-1} \mathbb{Q}_f \right|.$$

In the above equation, the factor on the right, $\mathcal{K}^{-1} \mathbb{Q}_f$, is exactly equal to \mathbb{Q}_Y , and thus lives on the simplex, which we denote by Δ . Using this fact and Hölder's inequality,

$$\left| \nu^\top \hat{\mathcal{K}}^{-1}(\hat{\mathcal{K}} - \mathcal{K})\mathcal{K}^{-1} \mathbb{Q}_f \right| \leq \sup_{q \in \Delta} \left| \nu^\top \hat{\mathcal{K}}^{-1}(\hat{\mathcal{K}} - \mathcal{K})q \right| \leq \left\| \nu^\top \hat{\mathcal{K}}^{-1} \right\|_1 \sup_{q \in \Delta} \left\| (\hat{\mathcal{K}} - \mathcal{K})q \right\|_\infty.$$

Next, we have

$$\sup_{q \in \Delta} \|(\hat{\mathcal{K}} - \mathcal{K})q\|_\infty = \max_{k \in [K]} \|\hat{\mathcal{K}}_k - \mathcal{K}_k\|_\infty,$$

where \mathcal{K}_k indexes the k -th column of \mathcal{K} . This yields the expression

$$\left\| \nu^\top \hat{\mathcal{K}}^{-1} \right\|_1 \sup_{q \in \Delta} \|(\hat{\mathcal{K}} - \mathcal{K})q\|_\infty = \left\| \nu^\top \hat{\mathcal{K}}^{-1} \right\|_1 \max_{k \in [K]} \|\hat{\mathcal{K}}_k - \mathcal{K}_k\|_\infty.$$

Putting everything together and going back to (15), we have

$$|\nu^\top \mathbb{Q}_Y - \nu^\top \hat{\mathbb{Q}}_Y| \leq \|\nu^\top \hat{\mathcal{K}}^{-1}\|_1 \left(\|\mathbb{Q}_f - \hat{\mathbb{Q}}_f\|_\infty + \max_{k \in [K]} \|\hat{\mathcal{K}}_k - \mathcal{K}_k\|_\infty \right). \quad (16)$$

Since $\|\nu^\top \hat{\mathcal{K}}^{-1}\|_1$ can be evaluated empirically, it remains to bound the distributional distances $\|\mathbb{Q}_f - \hat{\mathbb{Q}}_f\|_\infty$ and $\max_{k \in [K]} \|\hat{\mathcal{K}}_k - \mathcal{K}_k\|_\infty$.

For the first term, we can simply apply the DKWM inequality [29, 30], which gives

$$\|\mathbb{Q}_f - \hat{\mathbb{Q}}_f\|_\infty \leq \sqrt{\frac{2}{N} \log \frac{2}{\alpha - \delta}} \quad (17)$$

with probability $1 - (\alpha - \delta)$. See [31] for details.

For the second term, $\max_{k \in [K]} \|\widehat{\mathcal{K}}_k - \mathcal{K}_k\|_\infty$, since we only have n samples for estimation, we use a more adaptive concentration result. In particular, for each $l, k \in [K]$, $n(k)\widehat{\mathcal{K}}_{l,k}$ (conditional on the k -th column) follows a binomial distribution with $n(k)$ samples and success probability $\mathcal{K}_{l,k}$. Therefore, if we let

$$C_{l,k} = \left\{ p : n(k)\widehat{\mathcal{K}}_{l,k} \in \left(F_{\text{Binom}(n(k),p)}^{-1} \left(\frac{\delta}{2K^2} \right), F_{\text{Binom}(n(k),p)}^{-1} \left(1 - \frac{\delta}{2K^2} \right) \right) \right\},$$

where $F_{\text{Binom}(n(k),p)}$ denotes the Binomial CDF, then by a union bound:

$$P \left(\max_{k \in [K]} \|\widehat{\mathcal{K}}_k - \mathcal{K}_k\|_\infty \geq \max_{l,k \in [K]} \max_{p \in C_{l,k}} |\widehat{\mathcal{K}}_{l,k} - p| \right) \leq \delta. \quad (18)$$

Combining equations (16), (17) and (18) yields the final result.

C.9 Proof of Corollary B.1

The proof follows by instantiating the terms in Theorem 1. In particular, we have $\mathbb{E}[g_\theta(f_1)] = \theta - \mathbb{E}[f_1]$, and we use Hoeffding's inequality to form an interval for this term at level $\alpha - \delta$:

$$\mathbb{E}[g_\theta(f_1)] \in \mathcal{T}_{\alpha-\delta}(\theta) = \left(\theta - \frac{1}{N} \sum_{i=1}^N \tilde{f}_i \pm B \sqrt{\frac{2 \log(\frac{2}{\alpha-\delta})}{N}} \right).$$

Therefore, the condition $0 \in \mathcal{R}_\delta + \mathcal{T}_{\alpha-\delta}(\theta)$ becomes

$$0 \in (\mathcal{R}_\delta^l, \mathcal{R}_\delta^u) + \theta - \frac{1}{N} \sum_{i=1}^N \tilde{f}_i + \left(-B \sqrt{\frac{2 \log(\frac{2}{\alpha-\delta})}{N}}, B \sqrt{\frac{2 \log(\frac{2}{\alpha-\delta})}{N}} \right),$$

which after rearranging and simplifying is equivalent to

$$\theta \in \left(\frac{1}{N} \sum_{i=1}^N \tilde{f}_i - \mathcal{R}_\delta^u - B \sqrt{\frac{2 \log(\frac{2}{\alpha-\delta})}{N}}, \frac{1}{N} \sum_{i=1}^N \tilde{f}_i - \mathcal{R}_\delta^l + B \sqrt{\frac{2 \log(\frac{2}{\alpha-\delta})}{N}} \right).$$

C.10 Proof of Corollary B.2

The proof follows by instantiating the terms in Theorem 1. First, we have $\mathbb{E}[g_\theta(f_1)] = q - P(f_1 \leq \theta)$, and we use Hoeffding's inequality to form an interval for this term at level $\alpha - \delta$:

$$\mathbb{E}[g_\theta(f_1)] \in \mathcal{T}_{\alpha-\delta}(\theta) = \left(q - \frac{1}{N} \sum_{i=1}^N \mathbb{1} \{ \tilde{f}_i \leq \theta \} \pm \sqrt{\frac{\log(\frac{2}{\alpha-\delta})}{2N}} \right).$$

Therefore, the condition $0 \in \mathcal{R}_\delta(\theta) + \mathcal{T}_{\alpha-\delta}(\theta)$ becomes

$$0 \in (\mathcal{R}_\delta^l(\theta), \mathcal{R}_\delta^u(\theta)) + q - \frac{1}{N} \sum_{i=1}^N \mathbb{1} \{ \tilde{f}_i \leq \theta \} + \left(-\sqrt{\frac{\log(\frac{2}{\alpha-\delta})}{2N}}, \sqrt{\frac{\log(\frac{2}{\alpha-\delta})}{2N}} \right),$$

which after rearranging and simplifying is equivalent to

$$\frac{1}{N} \sum_{i=1}^N \mathbb{1} \{ \tilde{f}_i \leq \theta \} \in \left(q + \mathcal{R}_\delta^l(\theta) - \sqrt{\frac{\log(\frac{2}{\alpha-\delta})}{2N}}, q + \mathcal{R}_\delta^u(\theta) + \sqrt{\frac{\log(\frac{2}{\alpha-\delta})}{2N}} \right).$$

C.11 Proof of Corollary B.3

We instantiate the relevant terms in Theorem 1. We have $\mathbb{E}[g_\theta(X_1, f_1)] = \mathbb{E}\left[-X_1 f_1 + X_1 \frac{1}{1 + \exp(-X_1^\top \theta)}\right]$. Note that, because X_1 is coordinatewise bounded, and $Y_1, \frac{1}{1 + \exp(-X_1^\top \theta)} \in [0, 1]$, we have $|(g_\theta(X_1, f_1))_j| \leq 2B_j$ almost surely. Therefore, we can apply Hoeffding's inequality, together with a union bound, to get an interval for $\mathbb{E}[g_\theta(X_1, f_1)]$ at level $\alpha - \delta$:

$$\mathbb{E}[g_\theta(X_1, f_1)] \in \mathcal{T}_{\alpha-\delta}(\theta) = \left(\frac{1}{N} \sum_{i=1}^N \tilde{X}_i \left(\frac{1}{1 + \exp(-\tilde{X}_i^\top \theta)} - \tilde{f}_i \right) \pm \sqrt{\frac{8 \log(\frac{2d}{\alpha-\delta})}{N}} \mathbf{B} \right),$$

where $\mathbf{B} = (B_1, \dots, B_d)$. Since the rectifier has no dependence on θ , the condition $0 \in \mathcal{R}_\delta(\theta) + \mathcal{T}_{\alpha-\delta}(\theta)$ becomes

$$0 \in (\mathcal{R}_\delta^l, \mathcal{R}_\delta^u) + \frac{1}{N} \sum_{i=1}^N \tilde{X}_i \left(\frac{1}{1 + \exp(-\tilde{X}_i^\top \theta)} - \tilde{f}_i \right) + \left(-\sqrt{\frac{8 \log(\frac{2d}{\alpha-\delta})}{N}} \mathbf{B}, \sqrt{\frac{8 \log(\frac{2d}{\alpha-\delta})}{N}} \mathbf{B} \right),$$

which after rearranging and simplifying is equivalent to

$$\frac{1}{N} \sum_{i=1}^N \tilde{X}_i \left(\tilde{f}_i - \frac{1}{1 + \exp(-\tilde{X}_i^\top \theta)} \right) \in \left(\mathcal{R}_\delta^l - \sqrt{\frac{8 \log(\frac{2d}{\alpha-\delta})}{N}} \mathbf{B}, \mathcal{R}_\delta^u + \sqrt{\frac{8 \log(\frac{2d}{\alpha-\delta})}{N}} \mathbf{B} \right).$$

D Confidence intervals for the mean

We give an overview of off-the-shelf confidence intervals for the mean. We state the results for two observation models: first for the i.i.d. sampling model considered in the main body and then for the finite-population setting discussed in Appendix A. In both cases, we provide a construction with nonasymptotic guarantees and one with asymptotic guarantees.

For the nonasymptotic confidence intervals, we rely on the results of Waudby-Smith and Ramdas [27], specifically their Theorem 3 and Theorem 4. We opt for these results because of their strong practical performance, which is primarily driven by variance adaptivity. These results assume that the observed random variables are bounded within a known interval. Without loss of generality we assume that the observations are bounded in $[0, 1]$ (otherwise we can always normalize the observations to $[0, 1]$).

For the asymptotic confidence intervals, we rely on the central limit theorem (CLT) and its variant for sampling without replacement; see [32, 33] for classical references.

D.1 Inference with i.i.d. samples

In the following two results, assume that we observe $Z_1, \dots, Z_n \stackrel{\text{i.i.d.}}{\sim} \mathbb{P}$ and let $\mu = \mathbb{E}[Z_1]$.

Proposition D.1 (Nonasymptotic CI: Theorem 3 in [27]). *Assume $\text{supp}(\mathbb{P}) \subseteq [0, 1]$. Let*

$$\hat{\mu}_t = \frac{0.5 + \sum_{j=1}^t Z_j}{t+1}, \quad \hat{\sigma}_t^2 = \frac{0.25 + \sum_{j=1}^t (Z_j - \hat{\mu}_t)^2}{t+1}, \quad \lambda_t = \sqrt{\frac{2 \log(2/\alpha)}{n \hat{\sigma}_{t-1}^2}}.$$

For every $m \in [0, 1]$, define the supermartingale:

$$M_t(m) = \frac{1}{2} \max \left\{ \prod_{j=1}^t \left(1 + \min \left(\lambda_j, \frac{0.5}{m} \right) (Z_j - m) \right), \prod_{j=1}^t \left(1 - \min \left(\lambda_j, \frac{0.5}{1-m} \right) (Z_j - m) \right) \right\}.$$

Let

$$\mathcal{C} = \bigcap_{t=1}^n \{m \in [0, 1] : M_t(m) < 1/\alpha\}.$$

Then,

$$P(\mu \in \mathcal{C}) \geq 1 - \alpha.$$

Intuitively, the supermartingale $M_t(m)$ should be thought of as the amount of evidence against m being the true mean. That is, $M_t(m)$ being big suggests that m is unlikely to be the true mean, so the final confidence set is the collection of all m for which the amount of such evidence is small.

For large n , computing the intersection in the definition of \mathcal{C} can be intractable, so we conservatively choose a subsequence of $1, \dots, n$ for the computation.

Proposition D.2 (Asymptotic CI: CLT interval). *Assume \mathbb{P} has a finite second moment. Let*

$$\mathcal{C} = \left(\frac{1}{n} \sum_{i=1}^n Z_i \pm z_{1-\alpha/2} \frac{\hat{\sigma}}{\sqrt{n}} \right),$$

where $\hat{\sigma} = \sqrt{\frac{1}{n} \sum_{i=1}^n (Z_i - \frac{1}{n} \sum_{j=1}^n Z_j)^2}$. Then,

$$\liminf_{n \rightarrow \infty} P(\mu \in \mathcal{C}) \geq 1 - \alpha.$$

D.2 Inference on a finite population

In the following two results, we assume that there exists a *fixed* sequence Z_1, \dots, Z_N , and we observe $\{Z_i : i \in \mathcal{I}\}$, where $\mathcal{I} = \{i_1, \dots, i_n\}$ is a uniform random subset of $[N]$ with cardinality n . We let $\mu = \frac{1}{N} \sum_{i=1}^N Z_i$. For the asymptotic result, we assume that Z_1, \dots, Z_N is the first N entries of an infinite underlying sequence Z_1, Z_2, \dots .

Proposition D.3 (Nonasymptotic CI: Theorem 4 in [27]). *Assume $Z_i \in [0, 1]$, $i \in [N]$. Let*

$$\hat{\mu}_t = \frac{0.5 + \sum_{j=1}^t Z_{i_j}}{t+1}, \quad \hat{\sigma}_t^2 = \frac{0.25 + \sum_{j=1}^t (Z_{i_j} - \hat{\mu}_t)^2}{t+1}, \quad \lambda_t = \sqrt{\frac{2 \log(2/\alpha)}{n \hat{\sigma}_{t-1}^2}}.$$

For every $m \in [0, 1]$, define the supermartingale:

$$M_t(m) = \frac{1}{2} \max \left\{ \prod_{j=1}^t \left(1 + \min \left(\lambda_j, \frac{0.5}{\mu_t(m)} \right) (Z_{i_j} - \mu_t(m)) \right), \prod_{j=1}^t \left(1 - \min \left(\lambda_j, \frac{0.5}{1 - \mu_t(m)} \right) (Z_{i_j} - \mu_t(m)) \right) \right\},$$

where $\mu_t(m) = \frac{Nm - \sum_{j=1}^{t-1} Z_{i_j}}{N - t + 1}$ is the putative mean. Let

$$\mathcal{C} = \bigcap_{t=1}^n \{m \in [0, 1] : M_t(m) < 1/\alpha\}.$$

Then,

$$P(\mu \in \mathcal{C}) \geq 1 - \alpha.$$

Proposition D.4 (Asymptotic CI: CLT for sampling without replacement). *Let $\sigma^2 = \frac{1}{N} \sum_{i=1}^N (Z_i - \mu)^2$, and $\hat{\sigma}^2 = \frac{1}{n} \sum_{i \in \mathcal{I}} (Z_i - \hat{\mu})^2$. Assume that μ and σ have a limit and that $n/N \rightarrow p$ for some $p \in (0, 1)$. Let*

$$\mathcal{C} = \left(\frac{1}{n} \sum_{i \in \mathcal{I}} Z_i \pm z_{1-\alpha/2} \frac{\hat{\sigma}}{\sqrt{n}} \sqrt{\frac{N-n}{N}} \right).$$

Then,

$$\liminf_{n, N \rightarrow \infty} P(\mu \in \mathcal{C}) \geq 1 - \alpha.$$

E Experimental details

E.1 Forest cover experiment details

The machine-learning model given by [3] outputs forest-cover predictions at 30m resolution for 3192 data points. We correspond these by latitude and longitude with gold-standard data points labeled as one of `{deforestation, no deforestation}` from [2]. In the first step, we split off half of the data to train a histogram-based gradient boosting tree to predict deforestation labels from the forest-cover predictions. We take a random sample of $n = 100$ data points as the gold-standard data, and try to cover the true fraction of deforestation events on the $N = 1596$ remaining data points. We use Corollary A.1 and Proposition D.4 to produce the prediction-powered confidence interval and classical interval, and a standard binomial confidence interval for the imputation approach.

E.2 Relating protein structure and post-translational modifications

Model for predicting disorder. The predictive model f is a logistic regression model that maps relative solvent-accessible surface area (RSA) of each position, computed based on the AlphaFold-predicted structure, to a probability that the position is in an IDR. Following Bludau, Willems, Zeng, Strauss, Hansen, Tanzer, Karayel, Schulman, and Mann [4], the RSA was locally smoothed with a window of 5, 10, 15, 20, 25, 30, or 35 amino acids, and a sigmoid function was used to predict disorder from this smoothed RSA quantity. To fit the sigmoid, we used the data in [4] that had disorder labels but no PTM labels. The window size was chosen as the value that resulted in the lowest variance of the bias, $Y - f$, on this data.